CrossMark

*J. Fluid Mech.* (2017), *vol.* 833, *pp.* 131–163. © Cambridge University Press 2017 
doi:10.1017/jfm.2017.669

# Tilted incompressible Coriolis modes in spheroids

**D. J. Ivers**†

School of Mathematics and Statistics, University of Sydney, NSW 2006, Australia

(Received 20 February 2017; revised 11 August 2017; accepted 14 September 2017; first published online 2 November 2017)

The incompressible flow of a uniform fluid, which fills a rigid spheroid rotating about an arbitrary axis fixed in an inertial frame, is dominated at small Rossby and Ekman numbers by the rotation through the Coriolis force. The effects of rotation on the flow can be found by treating the Coriolis force modified by a pressure gradient as a skew-symmetric bounded linear operator $\mathcal{C}$ acting on smooth inviscid incompressible flows in the spheroid. It is shown that the space of incompressible polynomial flows of degree $N$ or less in the spheroid is invariant under $\mathcal{C}$ for any $N$. The skew symmetry of $\mathcal{C}$ implies the Coriolis operator $\mathcal{C}$ is non-defective for such flows with an orthogonal set of eigenmodes (inertial and geostrophic modes) which form a basis for the finite-dimensional space of spheroidal polynomial flows. The eigenmodes are tilted if the rotation axis is not aligned with the symmetry axis of the spheroid. The non-defective property of $\mathcal{C}$ enables enumeration of the modes and proof of their completeness using the Weierstrass polynomial approximation theorem. The fundamental tool, which is required to establish invariance of spheroidal polynomial flows under $\mathcal{C}$ and completeness of the Coriolis modes, is that the solution of the polynomial Poisson–Neumann problem, i.e. Poisson's equation with Neumann boundary condition and polynomial data, in a spheroid is a polynomial. The Coriolis modes of degree one and all geostrophic modes are explicitly constructed. Only the modes of degree one have non-zero angular momentum in the boundary frame.

**Key words:** geophysical and geological flows, rotating flows, waves in rotating fluids

## 1. Introduction

An incompressible fluid of uniform density filling a spheroidal volume $V$ with a rigid boundary $\partial V$, which rotates in an inertial frame in space $E^3$, can support internal inertial waves (Thomson 1880). Inertial waves occur in natural and laboratory flows in which the Coriolis force and inertia in the boundary frame dominate other forces. Inertial waves underlie many geophysical and astrophysical phenomena (see for example Greenspan 1968; Aldridge & Lumb 1987; Zhang 1993; Zhang *et al.* 2001). Inertial waves can generate a strong zonal flow through nonlinear interaction (Zhang & Liao 2004; Tilgner 2007) and may dissipate tidal energy in rotating giant planets (Ogilvie & Lin 2004). Magnetically modified inertial waves may explain some geomagnetic variations (Malkus 1967). Inertial waves can be excited experimentally

† Email address for correspondence: david.ivers@sydney.edu.au

https://doi.org/10.1017/jfm.2017.669 Published online by Cambridge University Press

by libration (Aldridge & Toomre 1969), thermal instabilities (Zhang 1994, 1995), precession (Gans 1970; Kerswell 1993; Lorenzani & Tilgner 2003; Zhang, Chan & Liao 2014), tides (Kerswell 1994; Tilgner 2007), planetary libration (Noir *et al.* 2009; Chan, Liao & Zhang 2011) and differential rotation (Kelley *et al.* 2007; Le Bars, Dizès & Le Gal 2007). Zhang & Liao (2017) is a comprehensive synthesis of applications of Coriolis modes to convection, oscillations and precession in contained rotating fluids.

If the boundary $\partial V$ rotates with angular velocity $\boldsymbol{\Omega}$ and acting on the flow are nonlinear advection, a gravitational–centripetal potential $U_e$, viscous and Poincaré forces and a magnetic Lorentz force $\boldsymbol{F}_L$ if the fluid is electrically conducting, then the momentum equation governing the fluid velocity $\boldsymbol{v}$ in the boundary frame is

$$\partial_t \boldsymbol{v} + \boldsymbol{\Omega} \times \boldsymbol{v} + \rho^{-1}\nabla p = \boldsymbol{F} := E\,\nabla^2 \boldsymbol{v} - \frac{1}{2} Ro\, \boldsymbol{v}\cdot\nabla\boldsymbol{v} - R\nabla U_e - Po\,\frac{\mathrm{d}\boldsymbol{\Omega}}{\mathrm{d}t}\times\boldsymbol{r} + El\,\rho^{-1}\boldsymbol{F}_L. \tag{1.1}$$

Length, time, speed, density $\rho$, pressure $p$ and force per unit mass are non-dimensionalised using a typical length $\mathcal{L}$, a typical inertial time $|2\boldsymbol{\Omega}_0|^{-1}$, a typical speed $\mathcal{V}$, a typical density $\rho_0$, $\rho_0|2\boldsymbol{\Omega}_0|\mathcal{V}\mathcal{L}$ and $\rho_0|2\boldsymbol{\Omega}_0|\mathcal{V}$. The dimensionless numbers, Ekman $E$, Rossby $Ro$, Poincaré $Po$, Elsasser $El$ and $R$ are typical magnitude ratios of the viscous, advective, Poincaré, Lorentz and gravitational forces to the Coriolis force.

If the flow is slow in the boundary fame, incompressible, inviscid and non-magnetic, a useful approximation is the rapid rotation state $E = Ro = R = Po = El = 0$, in which $\boldsymbol{\Omega}$ is constant and the density is homogeneous $\rho = 1$. The flow is dominated by the Coriolis force and consists of inertial waves and a steady geostrophic flow. Weak driving by advective, gravitational, viscous, Poincaré and Lorentz forces can be considered subsequently. The momentum and mass equations governing the solenoidal velocity $\boldsymbol{v}$ in the boundary frame reduce to

$$\partial_t \boldsymbol{v} + \widehat{\boldsymbol{\Omega}} \times \boldsymbol{v} + \nabla p = \boldsymbol{f}, \quad \nabla\cdot\boldsymbol{v} = 0, \tag{1.2a,b}$$

where $\widehat{\boldsymbol{\Omega}} := \boldsymbol{\Omega}/|\boldsymbol{\Omega}|$ is constant. The (dimensionless) volume force $\boldsymbol{f} = \boldsymbol{F} - \nabla p_F$ is the incompressible projection of $\boldsymbol{F}$, where the auxiliary pressure $p_F$ is chosen so that $\boldsymbol{f}$ satisfies

$$\nabla\cdot\boldsymbol{f} = 0 \quad \text{in } V; \quad \boldsymbol{n}\cdot\boldsymbol{f} = 0 \quad \text{on } \partial V. \tag{1.3a,b}$$

The normal flow vanishes on the boundary $\partial V$,

$$\boldsymbol{n}\cdot\boldsymbol{v} = 0. \tag{1.4}$$

In Cartesian coordinates with the $z$-axis aligned along the symmetry axis of $V$, the boundary $\partial V$ and its natural (non-unit) outward normal are

$$\frac{x^2+y^2}{a^2} + \frac{z^2}{c^2} = 1, \quad \boldsymbol{n} := \frac{x}{a^2}\boldsymbol{i} + \frac{y}{a^2}\boldsymbol{j} + \frac{z}{c^2}\boldsymbol{k}. \tag{1.5a,b}$$

The normal is a polynomial vector field of degree one defined everywhere in $E^3$. It is not assumed that the rotation is aligned with the symmetry axis of $V$, so that $\widehat{\boldsymbol{\Omega}} = \alpha\boldsymbol{i} + \beta\boldsymbol{j} + \gamma\boldsymbol{k}$, $\alpha^2+\beta^2+\gamma^2 = 1$, may be tilted from $\boldsymbol{k}$ with $\boldsymbol{k}\cdot\widehat{\boldsymbol{\Omega}} = \gamma = \cos\Theta$, where $\Theta$ is the tilt angle. Spheroidal geometries are useful approximations in planetary systems and nebulae (Tassoul 1978, § 4.4, Dermott 1979; Balick & Frank 2002; Thomas 2010; Chan *et al.* 2011; Zhang *et al.* 2014).

https://doi.org/10.1017/jfm.2017.669 Published online by Cambridge University Press

Free solutions ($\boldsymbol{f} = \boldsymbol{0}$) with $\partial \boldsymbol{v}/\partial t \neq 0$ are inertial waves, or inertial modes if they have a pure frequency; solutions with $\partial \boldsymbol{v}/\partial t = \boldsymbol{0}$ are geostrophic flows. Thomson (1880) determined the inertial modes in a cylinder and cylindrical shell rotating about their axes. Poincaré (1885) gave a partial derivation of the inertial modes for an ellipsoid rotating about a principal axis in terms of Lamé functions; see also Hough (1895, Appendix p. 479). In particular, Poincaré showed the inertial modes are polynomials in $x$, $y$, $z$. Bryan (1889) derived the aligned inertial modes for a fluid spheroid with a free surface rotating about its symmetry axis in terms of modified spheroidal harmonics. Kudlick (1966) and Zhang, Liao & Earnshaw (2004*b*) constructed explicit polynomial forms of the spheroidal inertial modes. In § 2 construction of the aligned inertial modes is outlined using coordinates introduced by Kudlick (1966, equations (4.4)). These coordinates are frequency dependent and degenerate at zero frequency but careful treatment of the frequency dependence allows construction of the spheroidal geostrophic modes in orthogonal polynomial form as the limit of the inertial modes at zero frequency. Liao & Zhang (2010*b*) derived explicit forms for the spherical geostrophic modes. A careful count of the dispersion relation zeros enumerates the aligned Coriolis (inertial and geostrophic) modes. In § 3 a basis is constructed, using a toroidal–poloidal representation of solenoidal fields in spheroids, for polynomial flows in a spheroid of degree $N$ or less for any $N$, which has the same number of elements as the aligned Coriolis modes of degree $N$ or less and allows enumeration of tilted Coriolis modes in § 6. The bases are also used to construct the Coriolis modes of degree one in § 3.2. These modes have the special property established in § 5.2 that they carry the angular momentum of a flow in the boundary frame. Zhang, Liao & Earnshaw (2004*a*) developed the asymptotic viscous theory of spheroidal inertial modes. In a numerical study of the aligned viscous spheroidal modes Schmitt (2006) computed the inviscid modes using the ingenious method of Schmitt & Jault (2004). The spheroidal toroidal–poloidal representation of § 3 can be used in numerical computations in spheroidal geometries such as the dynamo problem (Ivers 2017*b*). Coriolis modes in tri-axial ellipsoids have been computed numerically by Vantieghem (2014). Wentzel–Kramers–Brillouin–Jeffreys (WKBJ) approximations for inertial waves in axisymmetric volumes have been derived by Ivanov & Papaloizou (2010). Inertial waves in the quasi-geostrophic approximation, including viscous effects, have been computed by Maffei, Jackson & Livermore (2017) in spheroids.

The original motivation of this work and Ivers, Jackson & Winch (2015) was the remarkable result of Zhang *et al.* (2001) that for inertial modes $\boldsymbol{u}$ and $\boldsymbol{v}$,

$$\int_V \boldsymbol{u}^* \cdot \nabla^2 \boldsymbol{v} \, \mathrm{d}V = 0 \tag{1.6}$$

if $\boldsymbol{u} = \boldsymbol{v}$ and $V$ is a sphere. This result defied proof directly from (1.2) and (1.4). Importantly, Zhang *et al.* (2001) also reported the integral is strictly negative, if $\boldsymbol{u} = \boldsymbol{v}$ and $V$ is a plane layer, cylinder, cylindrical annulus or prism, with a proof for the annulus. See also Liao & Zhang (2010*a*). The result, however, is not restricted to a sphere, since Zhang *et al.* (2004*a*) later showed the integral vanishes if $\boldsymbol{u} = \boldsymbol{v}$ and $V$ is a spheroid, a result which is important in the asymptotic viscous theory. The crucial step for Ivers *et al.* (2015) and the present work was the result of Liao & Zhang (2009), that the integral vanishes if $V$ is a sphere and the polynomial degree of $\boldsymbol{v}$ is less than or equal to the polynomial degree of $\boldsymbol{u}$. This more general result, and the previous results of Zhang and his collaborators, suggested the approach of Ivers *et al.*

https://doi.org/10.1017/jfm.2017.669 Published online by Cambridge University Press

(2015) and the present work to restrict the Coriolis force to inviscid incompressible polynomial flows in $V$.

It is useful to introduce the space $\boldsymbol{\mathcal{V}}^k(V)$ of $C^k$ ($k$-times continuously differentiable) inviscid incompressible velocities in $V$, i.e. flows which satisfy (1.2*b*) and (1.4). Thus $\boldsymbol{\mathcal{V}}^k(V) := \{\boldsymbol{v} \in [C^k(V)]^3 \mid \boldsymbol{\nabla}\cdot\boldsymbol{v} = 0 \text{ in } V, \boldsymbol{n}\cdot\boldsymbol{v} = 0 \text{ on } \partial V\}$ with the inner-product

$$(\boldsymbol{v}_1, \boldsymbol{v}_2) := \int_V \boldsymbol{v}_1 \cdot \boldsymbol{v}_2^* \,\mathrm{d}V, \tag{1.7}$$

where the asterisk denotes complex conjugation and $C^k(V)$ is the space of complex-valued $C^k$ scalar functions on $V$. The associated norm is $\|\boldsymbol{v}\| = (\boldsymbol{v}, \boldsymbol{v})^{1/2}$, $(\boldsymbol{v}_1, \boldsymbol{v}_2) = (\boldsymbol{v}_2, \boldsymbol{v}_1)^*$ and the Cauchy–Schwartz inequality $|(\boldsymbol{v}_1, \boldsymbol{v}_2)| \leqslant \|\boldsymbol{v}_1\|\,\|\boldsymbol{v}_2\|$ holds. The flows have finite kinetic energy. The spatial structure of inertial modes in $V$ can be studied using the linear incompressible Coriolis operator $\boldsymbol{\mathcal{C}} : \boldsymbol{\mathcal{V}}^1(V) \longrightarrow \boldsymbol{\mathcal{V}}^1(V)$ (Ivers *et al.* 2015) defined by

$$\boldsymbol{\mathcal{C}}\boldsymbol{v} := \widehat{\boldsymbol{\Omega}} \times \boldsymbol{v} + \boldsymbol{\nabla} p, \tag{1.8}$$

where $\boldsymbol{\nabla}\cdot\boldsymbol{v} = 0$ in $V$ and $\boldsymbol{n}\cdot\boldsymbol{v} = 0$ on $\partial V$ since $\boldsymbol{v} \in \boldsymbol{\mathcal{V}}^1(V)$, and the pressure $p \in C^2(V)$ satisfies the elliptic Poisson–Neumann problem with consistent data,

$$\nabla^2 p = -\boldsymbol{\nabla}\cdot(\widehat{\boldsymbol{\Omega}} \times \boldsymbol{v}) \quad \text{in } V; \qquad \partial_n p = -\boldsymbol{n}\cdot\widehat{\boldsymbol{\Omega}} \times \boldsymbol{v} \quad \text{on } \partial V; \qquad \int_V p \,\mathrm{d}V = 0. \tag{1.9$a$–$c$}$$

The conditions (1.9) associate with each $\boldsymbol{v}$ a unique $p$ and ensure that $\boldsymbol{\mathcal{C}}\boldsymbol{v} \in \boldsymbol{\mathcal{V}}^1(V)$, i.e.

$$\boldsymbol{\nabla}\cdot(\boldsymbol{\mathcal{C}}\boldsymbol{v}) = 0 \quad \text{in } V, \qquad \boldsymbol{n}\cdot\boldsymbol{\mathcal{C}}\boldsymbol{v} = 0 \quad \text{on } \partial V. \tag{1.10$a$,$b$}$$

The operator $\boldsymbol{\mathcal{C}}$ is time independent.

The initial value problem consisting of (1.2) subject to (1.4) with $\boldsymbol{f} \in \boldsymbol{\mathcal{V}}^1(V)$ and $\boldsymbol{v}$ prescribed at $t = 0$ can be solved in principle by separating the time dependence and using spatial modes. Thus, if $\boldsymbol{f}(\boldsymbol{r}, t) = \boldsymbol{f}(\boldsymbol{r})\mathrm{e}^{-\lambda t}$, we assume the forcing is not resonant and $\lambda$ is not a defective eigenvalue of $\boldsymbol{\mathcal{C}}$ and consider a solution of (1.2) of the form $\boldsymbol{v}(\boldsymbol{r}, t) = \boldsymbol{v}(\boldsymbol{r})\mathrm{e}^{-\lambda t}$ with $p(\boldsymbol{r}, t) = p(\boldsymbol{r})\mathrm{e}^{-\lambda t}$. In terms of the angular frequency $\omega$ the decay rate $\lambda = \mathrm{i}\omega$. The momentum equation (1.2*a*) becomes

$$(\boldsymbol{\mathcal{C}} - \lambda)\boldsymbol{v} = \boldsymbol{f}, \tag{1.11}$$

noting (1.3) and (1.10). The velocity $\boldsymbol{v}$ can be isolated in (1.2*a*),

$$\lambda(1 + \lambda^2)\boldsymbol{v} = \lambda^2(\boldsymbol{\nabla} p - \boldsymbol{f}) + \lambda\widehat{\boldsymbol{\Omega}} \times (\boldsymbol{\nabla} p - \boldsymbol{f}) + \widehat{\boldsymbol{\Omega}}\cdot(\boldsymbol{\nabla} p - \boldsymbol{f})\widehat{\boldsymbol{\Omega}}, \tag{1.12}$$

and then eliminated using (1.2*b*) to yield the forced Poincaré equation,

$$\lambda^2\nabla^2 p + (\widehat{\boldsymbol{\Omega}}\cdot\boldsymbol{\nabla})^2 p = -\lambda\widehat{\boldsymbol{\Omega}}\cdot\boldsymbol{\nabla}\times\boldsymbol{f} + \widehat{\boldsymbol{\Omega}}\cdot\boldsymbol{\nabla}(\widehat{\boldsymbol{\Omega}}\cdot\boldsymbol{f}), \quad \text{in } V; \tag{1.13}$$

which is hyperbolic if $\lambda$ is imaginary and $|\lambda| < 1$, and the forced boundary condition,

$$\lambda^2\partial_n p + \lambda\boldsymbol{n}\times\widehat{\boldsymbol{\Omega}}\cdot\boldsymbol{\nabla} p + (\widehat{\boldsymbol{\Omega}}\cdot\boldsymbol{\nabla} p)\boldsymbol{n}\cdot\widehat{\boldsymbol{\Omega}} = \lambda\boldsymbol{n}\cdot\widehat{\boldsymbol{\Omega}}\times\boldsymbol{f} + \widehat{\boldsymbol{\Omega}}\cdot\boldsymbol{f}\boldsymbol{n}\cdot\widehat{\boldsymbol{\Omega}}, \quad \text{in } \partial V. \tag{1.14}$$

Poincaré's equation (1.13) must be solved subject to the boundary condition (1.14).

The Coriolis operator $\boldsymbol{\mathcal{C}}$ and its eigenmodes have the well-known properties listed in the following theorem. Proofs of (a)–(e) are given in Greenspan (1968) or Ivers *et al.* (2015); proof of (f) is immediate.

https://doi.org/10.1017/jfm.2017.669 Published online by Cambridge University Press

THEOREM 1.1. (a) *The operator* $\mathcal{C}$ *is bounded on* $\boldsymbol{\mathcal{V}}^1(V)$ *and continuous. In terms of the operator norm* $\|\mathcal{C}\|$ *of* $\mathcal{C}$ *defined by* $\|\mathcal{C}\| := \sup_{\boldsymbol{v}\neq\boldsymbol{0}} \|\mathcal{C}\boldsymbol{v}\|/\|\boldsymbol{v}\|$, $\|\mathcal{C}\| \leqslant 1$ *and* $\|\mathcal{C}\boldsymbol{v}\| \leqslant \|\boldsymbol{v}\|$.

(b) *The resolvent set* $\Gamma$ *of* $\mathcal{C}$ *contains* $\mathbb{C} \setminus [-\mathrm{i}, \mathrm{i}]$.

(c) *The operator* $\mathcal{C}$ *is skew symmetric* ($-\mathrm{i}\mathcal{C}$ *is symmetric), i.e.* $(-\mathrm{i}\mathcal{C}\boldsymbol{v}_1,\ \boldsymbol{v}_2) = (\boldsymbol{v}_1, -\mathrm{i}\mathcal{C}\boldsymbol{v}_2)$ *for all* $\boldsymbol{v}_1, \boldsymbol{v}_2 \in \boldsymbol{\mathcal{V}}^1(V)$.

(d) *The values* $\lambda = \pm\mathrm{i}$ *are not eigenvalues of* $\mathcal{C}$.

(e) *The eigenvalues* $\lambda$ *of* $\mathcal{C}$ *are imaginary, i.e. the frequencies are real, and* $|\lambda| \leqslant 1$*: and modes* $(\boldsymbol{v}_1, P_1, \lambda_1)$ *and* $(\boldsymbol{v}_2, P_2, \lambda_2)$ *with different eigenvalues (frequencies)* $\lambda_1 = \mathrm{i}\omega_1 \neq \lambda_2 = \mathrm{i}\omega_2$ *are orthogonal,* $(\boldsymbol{v}_1, \boldsymbol{v}_2) = 0$.

(f) *The operator* $\mathcal{C}$ *is real. Hence if* $(\boldsymbol{v}, P, \lambda)$ *is a eigenmode then* $(\boldsymbol{v}^*, P^*, \lambda^*)$ *is a eigenmode. Thus, if* $\omega$ *is an eigenfrequency,* $-\omega$ *is an eigenfrequency.*

The main result of the present work is that the Coriolis operator maps polynomial flows to polynomial flows of the same degree in a spheroid, even if $\boldsymbol{\Omega}$ is tilted from the symmetry axis. This result is established in § 4. It follows that tilted spheroidal Coriolis modes are polynomials. Tilted geostrophic modes are explicitly constructed in § 5. The results on dissipation integrals by Zhang *et al.* (2004*a*), Liao & Zhang (2009) and Ivers *et al.* (2015) are extended to spheroidal Coriolis modes in § 5.4.

The importance of completeness of Coriolis modes is emphasised by Zhang *et al.* (2004*a*) and by Zhang *et al.* (2014) for precession in spheroids. Coriolis modes are complete in periodic ducts (Cui, Zhang & Liao 2014), spheres (Ivers *et al.* 2015) and tri-axial ellipsoids (Backus & Rieutord 2017; Ivers 2017*a*). The approach of Backus & Rieutord (2017) is more abstract than Ivers (2017*a*). In § 6 it is shown that spheroidal Coriolis modes are complete for any tilt $\Theta$. There is a general completeness result for Coriolis modes in any bounded volume $V$ (Ivers *et al.* 2015), that $-\mathrm{i}\mathcal{C}$ can be extended to a bounded self-adjoint operator $-\mathrm{i}\overline{\mathcal{C}}$ on a Hilbert space of flows and by the spectral theorem for such operators any flow can be expanded as a Riemann–Stieltjes integral using the spectral resolution of $-\mathrm{i}\overline{\mathcal{C}}$. In general, the expansion requires a non-trivial integral over the continuous spectrum of $-\mathrm{i}\overline{\mathcal{C}}$, but for periodic ducts, spheres, spheroids and tri-axial ellipsoids it reduces to an infinite series over the discrete Coriolis modes. Dyson & Schutz (1979) have shown that the spatial adiabatic modes of differentially rotating axisymmetric perfect-fluid stellar models are complete, but in a more general sense which also requires the continuous spectrum. The axisymmetry of the basic state precludes application of their result to tilted Coriolis modes. Conclusions are given in § 7.

## 2. Aligned spheroidal Coriolis modes

Bryan (1889) explicitly constructed the spheroidal inertial modes if the rotation axis is aligned with the symmetry axis, i.e. $\widehat{\boldsymbol{\Omega}} = \mathbf{1}_z$. Explicit polynomial forms are derived in Kudlick (1966) and Zhang *et al.* (2004*b*). The Coriolis modes (inertial and geostrophic) are enumerated here by carefully counting the zeros of the dispersion relation, including multiplicities. A different argument is used in Theorem 4.4 to enumerate the Coriolis modes if the rotation is tilted from the symmetry axis. An orthogonal set of aligned spheroidal geostrophic pressure modes are also constructed by taking the limit $\omega \to 0$ of the inertial modes. These agree with Liao & Zhang (2010*b*) in the spherical limit $c \to a$.

https://doi.org/10.1017/jfm.2017.669 Published online by Cambridge University Press

### 2.1. *Spheroidal inertial pressure modes in aligned rotation*

The aligned spheroidal inertial ($\omega \neq 0$) modes can be found by solving Poincaré's equation (1.13) with $\boldsymbol{f} = \boldsymbol{0}$ subject to the boundary condition (1.14). Bryan (1889) following Poincaré (1885) transformed Poincaré's equation, by a (real or imaginary) change of scale in $z$, to Laplace's equation which can be solved in prolate or oblate spheroidal coordinates. A different auxiliary set of spheroidal coordinates is used to implement the boundary condition. The two sets of coordinates are confocal and therefore orthogonal, and their angular coordinates coincide (only) on the boundary. The present solution method is to transform the boundary spheroid to a sphere and map the aligned spheroidal problem to a spherical inertial mode problem with modified frequency and boundary condition. In Cartesian coordinates the free Poincaré equation (1.11) with $\boldsymbol{f} = \boldsymbol{0}$ and $\lambda = \mathrm{i}\omega$ is

$$\frac{\partial^2 P}{\partial x^2} + \frac{\partial^2 P}{\partial y^2} - \left(\frac{1}{\omega^2} - 1\right)\frac{\partial^2 P}{\partial z^2} = 0. \tag{2.1}$$

The scale transformation

$$\mathring{x} = x/a, \quad \mathring{y} = y/a, \quad \mathring{z} = z/c, \tag{2.2a–c}$$

maps the boundary spheroid $\partial V$ (1.5*a*) to the unit sphere $\mathring{x}^2 + \mathring{y}^2 + \mathring{z}^2 = 1$ and Poincaré's equation to

$$\frac{\partial^2 P}{\partial \mathring{x}^2} + \frac{\partial^2 P}{\partial \mathring{y}^2} - \left(\frac{1}{\mathring{\omega}^2} - 1\right)\frac{\partial^2 P}{\partial \mathring{z}^2} = 0, \tag{2.3}$$

if the modified frequency $\mathring{\omega}$ is defined by

$$\frac{1}{\mathring{\omega}^2} - 1 := \frac{a^2}{c^2}\left(\frac{1}{\omega^2} - 1\right). \tag{2.4}$$

Thus $|\omega| < 1$ from Theorem 1.1(f) implies $|\mathring{\omega}| < 1$; conversely, if $|\mathring{\omega}| < 1$, then $|\omega| < 1$; and $|\mathring{\omega}| = 1$ if and only if $|\omega| = 1$. Also $\mathring{\omega} = 0$ if and only if $\omega = 0$, since

$$\mathring{\omega}^2 := \frac{(1-e^2)\omega^2}{1 - e^2\omega^2}, \quad \omega^2 := \frac{\mathring{\omega}^2}{1 - e^2(1-\mathring{\omega}^2)}, \tag{2.5a,b}$$

where the oblate ellipticity $e := \sqrt{1 - c^2/a^2}$. See figure 1. If the spheroid is oblate $e^2 > 0$ and if prolate $e^2 < 0$. The prolate ellipticity is $e_p := \sqrt{1 - a^2/c^2}$, $(1-e^2)(1-e_p^2) = 1$ and $e^2 = -e_p^2/(1-e_p^2)$. Note that there is no distinction between the oblate and prolate cases in the derivation in this section.

In cylindrical polar coordinates $(s, \phi, z)$ the boundary spheroid (1.5*a*) is $s^2/a^2 + z^2/c^2 = 1$ which, under the scale transformation (2.2), becomes the unit sphere $\mathring{s}^2 + \mathring{z}^2 = 1$, where $\mathring{s} = \sqrt{\mathring{x}^2 + \mathring{y}^2} = s/a$. Thus from the spherical case (see Ivers *et al.* 2015) the solutions of Poincaré's equation are

$$P = P^m_{n,\omega} := P^m_n(\zeta_{\mathring{\omega}})\, P^m_n(\xi_{\mathring{\omega}})\mathrm{e}^{\mathrm{i}m\phi}, \tag{2.6}$$

where $(\xi, \zeta, \phi)$ are non-orthogonal frequency-dependent spheroidal coordinates (attributed to Greenspan by Kudlick 1966, equation (4.2)), which are related to scaled cylindrical polar coordinates $(\mathring{s}, \phi, \mathring{z})$ by

$$\mathring{\sigma}\mathring{s} = \sqrt{1-\zeta^2}\sqrt{1-\xi^2}, \quad \mathring{\omega}\mathring{z} = \xi\zeta, \quad \mathring{\sigma}^2 = 1 - \mathring{\omega}^2. \tag{2.7a–c}$$

https://doi.org/10.1017/jfm.2017.669 Published online by Cambridge University Press

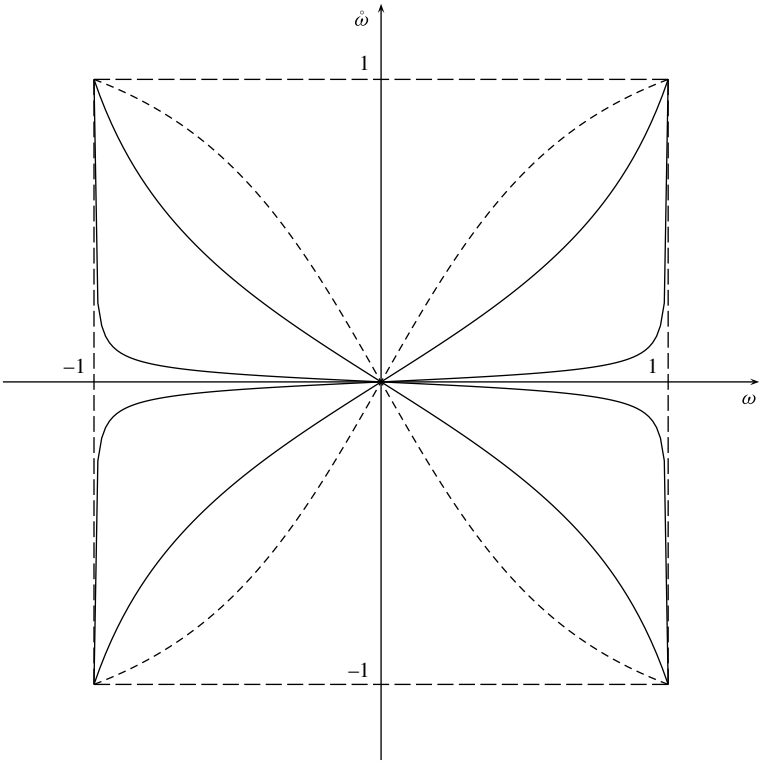



FIGURE 1. Plot of $\mathring{\omega}$ versus $\omega$ for $e = 0.8$, 0.999 and $e_p = 0.8$ (dashed). By (2.5) the diagram is reflected in the diagonals $\mathring{\omega} = \pm\omega$ if $a$ and $c$ are interchanged; this also swaps $e$ and $e_p$. As $e \uparrow 1$ the solid curves are squeezed against the asymptotes $\omega = \pm 1$ and $\mathring{\omega} = 0$; as $e_p \uparrow 1$ the dashed curves are squeezed against the asymptotes $\mathring{\omega} = \pm 1$ and $\omega = 0$; see Kudlick (1966, pp. 37, 38).

In terms of unscaled cylindrical polar coordinates, $\mathring{\sigma} s = a\sqrt{1-\zeta^2}\sqrt{1-\xi^2}$ and $\mathring{\omega} z = c\xi\zeta$. The element of arc length is given by

$$\begin{aligned} \mathrm{d}\ell^2 \;=\; & \left(\frac{a^2}{\mathring{\sigma}^2}\frac{1-\zeta^2}{1-\xi^2}\xi^2 + \frac{c^2}{\mathring{\omega}^2}\zeta^2\right)\mathrm{d}\xi^2 + \left(\frac{a^2}{\mathring{\sigma}^2} + \frac{c^2}{\mathring{\omega}^2}\right) 2\xi\zeta\,\mathrm{d}\xi\,\mathrm{d}\zeta \\ & + \left(\frac{a^2}{\mathring{\sigma}^2}\frac{1-\xi^2}{1-\zeta^2}\zeta^2 + \frac{c^2}{\mathring{\omega}^2}\xi^2\right)\mathrm{d}\zeta^2 + s^2\,\mathrm{d}\phi^2. \end{aligned} \tag{2.8}$$

In (2.6) $P_n^m$ is the associated Legendre function of degree $n$ and order $m$, $m \in \mathbb{Z}$, $|m| \leqslant n$, $\mathring{\omega} \neq 0$ and the $\mathring{\omega}$ dependence of $\zeta$ and $\xi$ is indicated.

The spheroidal inertial mode $P_{n,\omega}^m$ is a polynomial in $s$ and $z$ of degree $n$ with a $\phi$-dependent factor $\mathrm{e}^{\mathrm{i}m\phi}$ and a polynomial in $x, y, z$ of degree $n$ (Kudlick 1966; Zhang *et al.* 2001). In fact, from Ivers *et al.* (2015)

$$P_{n,\omega}^m = \begin{cases} (\mathring{\sigma}\mathring{s}\mathrm{e}^{\mathrm{i}\phi})^m(\mathring{\omega}\mathring{z})^q U_n^m(\mathring{\sigma}^2\mathring{s}^2, \mathring{\omega}^2 z^2), & \text{if } m \geqslant 0; \\ (\mathring{\sigma}\mathring{s}\mathrm{e}^{-\mathrm{i}\phi})^{|m|}(\mathring{\omega}\mathring{z})^q U_n^m(\mathring{\sigma}^2\mathring{s}^2, \mathring{\omega}^2\mathring{z}^2), & \text{if } m < 0; \end{cases} \tag{2.9}$$

where $q := n - |m| \pmod 2$ is either 0 or 1, and $U_n^m(\mathring{\sigma}^2\mathring{s}^2, \mathring{\omega}^2\mathring{z}^2)$ is polynomial in $\mathring{\sigma}^2\mathring{s}^2$ and $\mathring{\omega}^2\mathring{z}^2$ of degree $(n - |m| - q)/2$. Expressions (2.9) are polynomials in $\mathring{x}, \mathring{y}, \mathring{z}$ since

https://doi.org/10.1017/jfm.2017.669 Published online by Cambridge University Press

$\mathring{s}\mathrm{e}^{\pm\mathrm{i}\phi} = \mathring{x} \pm \mathrm{i}\mathring{y}$. The polynomial properties in $s$, $z$ and in $x$, $y$, $z$ follow from $\mathring{s} = s/a$ and (2.2). The $z$-parity of $P^m_{n,\omega}$ is determined by $q$.

### 2.2. *Frequencies of aligned Coriolis modes*

In cylindrical coordinates $(s, \phi, z)$ the normal (1.5*b*) is $\boldsymbol{n} = s\mathbf{1}_s/a^2 + z\mathbf{1}_z/c^2$, and the boundary condition (1.14) becomes in terms of $(\mathring{s}, \phi, \mathring{z})$,

$$\mathring{\omega}^2\mathring{s}\,\partial_{\mathring{s}}P + (\mathring{\omega}/\omega)\mathrm{i}\mathring{\omega}\partial_\phi P - (1-\mathring{\omega}^2)\mathring{z}\,\partial_{\mathring{z}}P = 0. \tag{2.10}$$

Equation (2.10) differs from the spherical case by the factor $\mathring{\omega}/\omega$ in the $\phi$-derivative term. The boundary condition is transformed to spheroidal coordinates using the following transformations for the first derivatives,

$$\partial_{\mathring{s}}P = \frac{\xi\,\partial_\xi P - \zeta\,\partial_\zeta P}{\mathring{\omega}J}, \quad \partial_{\mathring{z}}P = \frac{\zeta(1-\xi^2)\partial_\xi P}{\mathring{\sigma}^2\mathring{s}J} - \frac{\xi(1-\zeta^2)\partial_\zeta P}{\mathring{\sigma}^2\mathring{s}J}, \tag{2.11$a$,$b$}$$

where $J = \partial(\mathring{s}, \mathring{z})/\partial(\xi, \zeta) = (\zeta^2 - \xi^2)/(\mathring{\omega}\mathring{\sigma}^2\mathring{s})$. The boundary $\mathring{s}^2 + \mathring{z}^2 = 1$ is given by $\mathring{s} = \sin\theta$, $\mathring{z} = \cos\theta$ or in the spheroidal coordinates $(\xi, \zeta, \phi)$ by $\xi = \cos\theta$, $\zeta = \mathring{\omega}$. Thus, using (2.11) the boundary condition (2.10) becomes $\mathring{\sigma}^2\partial_\zeta P - (\mathring{\omega}/\omega)\mathrm{i}\partial_\phi P = 0$. Substituting the separable solution (2.6) gives $P^m_n(\xi)(\mathring{\sigma}^2\partial_\zeta + m\mathring{\omega}/\omega)P^m_n(\zeta) = 0$ on $\xi = \cos\theta$, $\zeta = \mathring{\omega}$. Since $\theta$ is arbitrary, $\mathring{\omega}$ is a zero of the dispersion relation,

$$(1-\mathring{\omega}^2)\frac{\mathrm{d}P^m_n(\mathring{\omega})}{\mathrm{d}\mathring{\omega}} + \frac{m\mathring{\omega}}{\omega}P^m_n(\mathring{\omega}) = 0. \tag{2.12}$$

Using the relation (2.5) between $\omega$ and $\mathring{\omega}$ condition (2.2) becomes

$$(1-\mathring{\omega}^2)\frac{\mathrm{d}P^m_n(\mathring{\omega})}{\mathrm{d}\mathring{\omega}} + m\sqrt{1-e^2(1-\mathring{\omega}^2)}P^m_n(\mathring{\omega}) = 0. \tag{2.13}$$

Now (Ivers *et al.* 2015), $P^m_n(\mathring{\omega}) = c^m_n(1-\mathring{\omega}^2)^{|m|/2}\prod_{k=1}^{n-|m|}(\mathring{\omega} - \mathring{\omega}_k)$, where $\mathring{\omega}_k$ for $k = 1:$ $n-|m|$ are the $n-|m|$ distinct zeros of $P^m_n(\mathring{\omega})$ on $(-1, 1)$ and $c^m_n$ is a constant. The frequency equation (2.13) can be written as

$$\frac{\mathrm{d}\ln P^m_n(\mathring{\omega})}{\mathrm{d}\mathring{\omega}} = \frac{\frac{1}{2}|m|}{\mathring{\omega}+1} + \frac{\frac{1}{2}|m|}{\mathring{\omega}-1} + \sum_{k=1}^{n-|m|}\frac{1}{\mathring{\omega}-\mathring{\omega}_k} = \sqrt{1-e^2(1-\mathring{\omega}^2)}\left[\frac{\frac{1}{2}m}{\mathring{\omega}-1} - \frac{\frac{1}{2}m}{\mathring{\omega}+1}\right]. \tag{2.14}$$

If $m > 0$ rearranging the second equation in (2.14) gives

$$\sum_{k=1}^{n-|m|}\frac{1}{\mathring{\omega}-\mathring{\omega}_k} = -\frac{\frac{1}{2}m[1+\sqrt{1-e^2(1-\mathring{\omega}^2)}]}{\mathring{\omega}+1} + \frac{\frac{1}{2}me^2(\mathring{\omega}+1)}{1+\sqrt{1-e^2(1-\mathring{\omega}^2)}} < 0. \tag{2.15}$$

The expression on the right-hand side is: monotonic in $|\mathring{\omega}| < 1$ for fixed $0 \leqslant e^2 < 1$ (oblate) or for $-\infty < e^2 \leqslant 0$ (prolate); tends to $-\infty$ as $\mathring{\omega} \to -1+$ or to $-(1/2)m$ $(1-e^2)$ as $\mathring{\omega} \to 1-$; and is monotonic in $-\infty < e^2 < 1$ for fixed $\mathring{\omega}$. For $m < 0$ the signs of the terms on the right-hand side of (2.15) are changed and $\mathring{\omega}$ is replaced by $-\mathring{\omega}$. Figure 2 shows a schematic plot of the two sides of the second equation in (2.15) for $n-|m| = 4$. For $m \neq 0$ this equation has $n-|m|$ zeros; for $m = 0$ there are $n-1$ zeros. The zeros are not symmetrically distributed about $\mathring{\omega} = 0$ but they are reasonably

https://doi.org/10.1017/jfm.2017.669 Published online by Cambridge University Press

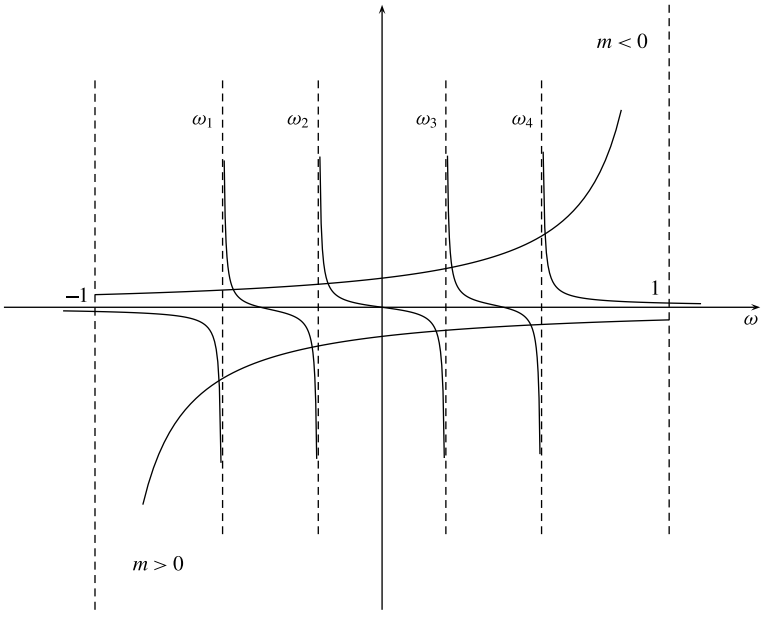



FIGURE 2. Schematic plot of (2.16) and the $m>0$ analogue for inertial frequencies $\omega$ with $n-|m|=4$. The right side curves are labelled by $m>0$ and $m<0$; as $e^2\uparrow 1$ these curves move toward the $\omega$ axis; and away from the $\omega$ axis as $e^2\downarrow -\infty$. The $m=0$ curve is the $\omega$ axis.

uniformly distributed on $[-1, 1]$. Thus for extremely oblate (prolate) spheroids with $e\approx 1$ ($e_p\approx 1$) the real frequencies are clustered near $\omega=\pm 1$ ($\omega=0$); see figure 2. This result was inferred from computations by Kudlick (1966). Geostrophic modes $\mathring{\omega}=0$ occur if and only if $m=0$ and $n$ is even. There are no $m=\pm n$ modes: in fact, the dispersion relation gives $\mathring{\omega}=1$ $(-1)$ for $m>0$ $(<0)$ in these cases. Thus we label the non-zero frequencies for $0<m\leqslant n-1$ by $\mathring{\omega}^m_{n,j}$ $(\omega^m_{n,j})$, where $j\in\mathbb{Z}$, $j\neq 0$ and $j=-(n-m+1)/2:(n-m-1)/2$, if $n-m$ is odd, or $j=-(n-m)/2:(n-m)/2$ if $n-m$ is even. The zero frequencies are $\mathring{\omega}^0_{n,0}$, where $n$ is even, $m=0$ and $j=0$. For $-(n-1)\leqslant m<0$, $\mathring{\omega}^m_{n,j}=\mathring{\omega}^{-m}_{n,-j}$ $(\omega^m_{n,j}=\omega^{-m}_{n,-j})$. We define the associated inertial pressure mode for the non-zero frequency $\omega^m_{n,j}$ by

$$P^m_{n,j}:=P^m_{n,\omega^m_{n,j}}. \tag{2.16}$$

Note that $P^m_{n,j}=P^{-m*}_{n,-j}$. The aligned geostrophic modes are constructed in § 2.3.

The number of Coriolis pressure modes of degree $N+1$ or less, which equals the number of Coriolis velocity modes of degree $N$ or less, is

$$C_N=\tfrac{1}{6}N(N+1)(2N+7), \tag{2.17}$$

as (expectedly) in the spherical case. For $N=1, 2$ there are 3, 11 modes and for $N\gg 1$ $C_N\approx N^3/3$.

### 2.3. *Aligned geostrophic pressure modes*

The natural aligned geostrophic modes, which are hierarchical in polynomial degree, can be constructed by taking the limit $\omega\to 0$ of the aligned inertial modes (2.7), as in the spherical case.

https://doi.org/10.1017/jfm.2017.669 Published online by Cambridge University Press

LEMMA 2.1. *For $m = 0$ and $\omega \to 0$ the solutions (2.6) reduce to the geostrophic modes,*

$$P^0_{n,0}(s) = P_n(0)P_n(\sqrt{1 - s^2/a^2}) - [P_n(0)]^2, \tag{2.18}$$

*where $n$ is even. $P^0_{n,0}(s)$ is a polynomial of even degree $n$ in $s$ and $P_n$ is the Legendre polynomial of degree $n$. As $s \to a$, $P^0_{n,0}(s) \to 0$. In terms of Jacobi polynomials $P^0_{n,0}(s) = (-)^{n/2}P_n(0)P^{(-1/2,0)}_{n/2}(2s^2/a^2 - 1) - [P_n(0)]^2$.*

*Proof.* From (2.7) $\xi^2 + \zeta^2 = 1 - \mathring{\sigma}^2\mathring{s}^2 + (\xi\zeta)^2 = 1 - \mathring{\sigma}^2\mathring{s}^2 + \mathring{\omega}^2\mathring{z}^2$. Thus as $\omega \to 0$, $\mathring{\omega} \to 0$ by (2.5) and $\xi^2 + \zeta^2 \to 1 - \mathring{s}^2 = 1 - s^2/a^2$. Further, by rearranging the binomial expansion of $(\xi^2 + \zeta^2)^l$ into the form,

$$\xi^{2l} + \zeta^{2l} = (\xi^2 + \zeta^2)^l - \sum_{j=1}^{\lfloor (l-1)/2 \rfloor} {}^lC_j(\xi\zeta)^{2j}(\xi^{2(l-2j)} + \zeta^{2(l-2j)}), \tag{2.19}$$

$\xi^{2l} + \zeta^{2l} \to (\xi^2 + \zeta^2)^l$, since $\mathring{\sigma} \to 1$ and $(\xi\zeta)^2 = \mathring{\omega}^2\mathring{z}^2 \to 0$. If $n$ is even, $P_n(z) = \sum_{k=0}^{n/2} p_{n,2k}z^{2k}$, where the $p_{n,2k}$ are constants, and

$$P_n(\xi)P_n(\zeta) = p_{n,0}\left[\sum_{k=0}^{n/2} p_{n,2k}(\xi^{2k} + \zeta^{2k}) - p_{n,0}\right] + (\xi\zeta)^2 \sum_{k=1}^{n/2}\sum_{l=1}^{n/2} p_{n,2k}p_{l,2k}\xi^{2(k-1)}\zeta^{2(l-1)}. \tag{2.20}$$

The double sum is $O(\xi\zeta)^2$. Thus for $n$ even, $P_n(\xi)P_n(\zeta) \to P^0_{n,0}$ in (2.18) as $\omega \to 0$, since $p_{n,0} = P_n(0)$. If $n$ is odd, $P_n(\xi)P_n(\zeta) \to 0$ as $\omega \to 0$. □

The modes (2.18) are orthogonal, for evaluating the inner product $(\boldsymbol{v}_1, \boldsymbol{v}_2)$ of two geostrophic modes gives

$$(\boldsymbol{v}_1, \boldsymbol{v}_2) = \int_V \nabla P_1 \cdot \nabla P_2^* \, \mathrm{d}V, \tag{2.21}$$

noting $n_1$ and $n_2$ are even and substituting $v^2 = 1 - s^2/a^2$ yields, apart from the factor $P_{n_1}(0)P_{n_2}(0)$,

$$\int_V \nabla P_{n_1}(\sqrt{1 - s^2/a^2}) \cdot \nabla P_{n_2}(\sqrt{1 - s^2/a^2}) \, \mathrm{d}V = 2\pi c \int_{-1}^{1} P'_{n_1}(v)(1 - v^2)P'_{n_2}(v) \, \mathrm{d}v. \tag{2.22}$$

An integration by parts and Legendre's differential equation shows the last integral vanishes if $n_1 \neq n_2$.

### 2.4. *Aligned velocity modes*

The velocity modes are constructed from the pressure modes using (3.9). Thus associated with the pressure mode $P^m_{n+1,j}$ is the velocity mode $\boldsymbol{v}^m_{n,j}$. Define

$$\boldsymbol{v}^m_n(\omega) := \begin{cases} \dfrac{\mathrm{i}\omega}{1 - \omega^2}(\nabla P^m_{n+1,\omega} - \omega^{-2}\widehat{\boldsymbol{\Omega}}\,\widehat{\boldsymbol{\Omega}} \cdot \nabla P^m_{n+1,\omega}) + \dfrac{1}{1 - \omega^2}\widehat{\boldsymbol{\Omega}} \times \nabla P^m_{n+1,\omega}, & \omega \neq 0; \\ \widehat{\boldsymbol{\Omega}} \times \nabla P^0_{n+1,0}(s), \quad m = 0, n \text{ odd}; \quad \omega = 0. \end{cases} \tag{2.23}$$

https://doi.org/10.1017/jfm.2017.669 Published online by Cambridge University Press

The Coriolis velocity modes are thus

$$\boldsymbol{v}^m_{n,j} := N^m_{n,j}\boldsymbol{v}^m_n(\omega^m_{n+1,j}), \quad |m| \leqslant n, \tag{2.24}$$

where $j = -(n-m+1)/2 : (n-m-1)/2$ if $n-m$ is odd, $j = -(n-m)/2 : (n-m)/2$ if $n-m$ is even and $j \neq 0$ unless $m = 0$ and $n$ is odd. The normalisation constant $N^m_{n,j} > 0$ is chosen so that the mode is normalised to $(\boldsymbol{v}^m_{n,j}, \boldsymbol{v}^m_{n,j}) = 1$. The complex conjugate $\boldsymbol{v}^{m*}_{n,j} = \boldsymbol{v}^{-m}_{n,-j}$ in agreement with Theorem 1.1(f). No modes $\boldsymbol{v}^m_{n,\omega}$ arise from $m = n+1$, i.e. $P^{\pm(n+1)}_{n+1}$. For $m \neq 0$ the associated inertial waves propagate eastward (westward) if $j > 0$ ($j < 0$). Equatorial symmetries are determined by $n-m$: the velocity modes are quadrupole symmetric if $n - m = 0 \,(\mathrm{mod}\ 2)$ and dipole symmetric if $n - m = 1 \,(\mathrm{mod}\ 2)$; and rotational symmetries about $\widehat{\boldsymbol{\Omega}}$ are determined by $m$. In terms of Jacobi polynomials their $\phi$-components can be written as

$$v^0_{2n-1,0} = N^0_{2n-1,0}\frac{\mathrm{d}P^0_{2n,0}(s)}{\mathrm{d}s} = N^0_{2n-1,0}(-)^n(2n+1)P_{2n}(0)sP^{(1/2,1)}_n(2s^2/a^2-1)/a^2. \tag{2.25}$$

Spheroidal Coriolis modes, which are all polynomial flows (see Theorem 6.2), are labelled below using a Greek letter, e.g. $\boldsymbol{v}_\alpha$; the degree of $\boldsymbol{v}_\alpha$ is denoted by $\deg\alpha$ and the angular frequency by $\omega_\alpha$. For aligned modes the Greek letter denotes a three index, e.g. $\boldsymbol{v}_\alpha \equiv \boldsymbol{v}^{m_\alpha}_{n_\alpha j_\alpha}$. For tilted modes the three-index interpretation fails but it can be interpreted as a two index: the first index indicates the polynomial degree of the mode and the second labels its frequency.

## 3. Polynomial flows in a spheroid

Let $\mathcal{P}_N$ denote the set of complex polynomials in $(x, y, z)$ of degree $N$. The space $\mathcal{P}_N$ is a finite-dimensional complex vector space of dimension $(1/6)N(N+1)(2N+1)$. Define the space of (inviscid) complex polynomial flows of degree $N$ on $V$, $\boldsymbol{\mathcal{P}}_N(V) = \{\boldsymbol{v} \in \mathcal{P}^3_N \mid \boldsymbol{\nabla}\cdot\boldsymbol{v} = 0 \text{ in } V, \boldsymbol{n}\cdot\boldsymbol{v} = 0 \text{ on } \partial V\}$ with inner product (1.11). It is shown later using Theorem 4.4 that aligned spheroidal Coriolis modes can also be enumerated using a basis of $\boldsymbol{\mathcal{P}}_N(V)$. This enumeration does not rely on explicit construction of the modes and so also works for tilted modes. The dimension of $\mathcal{P}^3_N$ is $(N+1)^3$. A typical element $\boldsymbol{v} \in \boldsymbol{\mathcal{P}}_N(V)$ can be written as $\boldsymbol{v} = \sum_{j+k+l\leqslant N}(v^{jkl}_x\boldsymbol{i} + v^{jkl}_y\boldsymbol{j} + v^{jkl}_z\boldsymbol{k})x^jy^kz^l$, As in the spherical case, constructing or even enumerating a basis of $\boldsymbol{\mathcal{P}}_N(V)$ from linear combinations of the power basis $\{x^iy^jz^k\boldsymbol{i}, x^iy^jz^k\boldsymbol{j}, x^iy^jz^k\boldsymbol{k}\}$, $i, j, k \in \mathbb{N}$ and $i+j+k \leqslant N$, of $\mathcal{P}^3_N$ is difficult due to the solenoidal condition and particularly the boundary condition (1.4). It is much simpler to construct a basis for $\boldsymbol{\mathcal{P}}_N(V)$ using spheroidal toroidal and poloidal fields. Alternative constructions of polynomial bases have been given by Lebovitz (1989) using the Lagrangian displacement and by Wu & Roberts (2011) using the vorticity.

### 3.1. *A spheroidal toroidal–poloidal basis*

Introduce the homoeoidal spheroidal coordinates $(r, \theta, \phi)$ in dimensionless form,

$$x = ar\sin\theta\cos\phi, \quad y = ar\sin\theta\sin\phi, \quad z = cr\cos\theta. \tag{3.1a–c}$$

Let $\boldsymbol{e}_r := \partial_r\boldsymbol{r}$, $\boldsymbol{e}_\theta := \partial_\theta\boldsymbol{r}/r$, $\boldsymbol{e}_\phi := \partial_\phi\boldsymbol{r}/r\sin\theta$ and let the velocity $\boldsymbol{v} = v_r\boldsymbol{e}_r + v_\theta\boldsymbol{e}_\theta + v_\phi\boldsymbol{e}_\phi$. Define a class of spheroidal toroidal and poloidal fields

$$\boldsymbol{T}\{t\} := \boldsymbol{e}_\theta\frac{\partial_\phi t}{\sin\theta} - \boldsymbol{e}_\phi\partial_\theta t, \quad \boldsymbol{S}\{s\} := -\boldsymbol{e}_r\frac{\mathring{\Lambda}^2 s}{r} + \boldsymbol{e}_\theta\frac{\partial_\theta\partial_r(rs)}{r} + \boldsymbol{e}_\phi\frac{\partial_\phi\partial_r(rs)}{r\sin\theta}, \tag{3.2a,b}$$

https://doi.org/10.1017/jfm.2017.669 Published online by Cambridge University Press

where $\mathring{\Lambda}^2 s := (\sin\theta)^{-1}\partial_\theta(\sin\theta\,\partial_\theta s) + (\sin\theta)^{-2}\partial_\phi\partial_\phi s$. Throughout the present § 3, $s$ and $t$ are the poloidal and toroidal potentials, not the cylindrical radius and the time. These fields are solenoidal identically in $t$ and $s$, $\boldsymbol{\nabla}\cdot\boldsymbol{T}\{t\} = 0$ and $\boldsymbol{\nabla}\cdot\boldsymbol{S}\{s\} = 0$, and any incompressible velocity can be represented as a sum of spheroidal toroidal and poloidal fields, $\boldsymbol{v} = \boldsymbol{S}\{s\} + \boldsymbol{T}\{t\}$, and the impenetrable boundary condition (2.9) becomes

$$s = 0, \quad \text{at } r = 1. \tag{3.3}$$

The streamlines of the toroidal flow $\boldsymbol{T}\{t\}$ are given by the level contours of $t$ on the surfaces of constant $r$ which are nested homoeoidal spheroids.

Scale the Cartesian coordinates $\mathring{x} = x/a$, $\mathring{y} = y/a$ and $\mathring{z} = z/c$, and the velocity,

$$\mathring{\boldsymbol{r}} = \boldsymbol{L}\cdot\boldsymbol{r} = \boldsymbol{r}\cdot\boldsymbol{L}, \quad \mathring{\boldsymbol{v}} = \boldsymbol{L}\cdot\boldsymbol{v} = \boldsymbol{v}\cdot\boldsymbol{L}, \tag{3.4a,b}$$

where $\mathring{\boldsymbol{r}} := \mathring{x}\boldsymbol{i} + \mathring{y}\boldsymbol{j} + \mathring{z}\boldsymbol{k}$ is the position vector in $(\mathring{x}, \mathring{y}, \mathring{z})$-space $\mathring{E}^3$, the diagonal scale tensor $\boldsymbol{L} := a^{-1}(\boldsymbol{ii} + \boldsymbol{jj}) + c^{-1}\boldsymbol{kk}$ with inverse $\boldsymbol{L}^{-1} := a(\boldsymbol{ii} + \boldsymbol{jj}) + c\boldsymbol{kk}$. Let $\mathring{\mathcal{P}}_N$ denote the set of complex polynomials in $(\mathring{x}, \mathring{y}, \mathring{z})$ of degree $N$. If $f(\boldsymbol{r}) \in \mathcal{P}_N$ then $f(\boldsymbol{L}^{-1}\cdot\mathring{\boldsymbol{r}}) \in \mathring{\mathcal{P}}_N$ and conversely. Let $\mathring{V} := \{\mathring{\boldsymbol{r}} \in \mathring{E}^3 \mid r = |\mathring{\boldsymbol{r}}| \leqslant 1\}$. Define the space of (inviscid) complex polynomial flows of degree $N$ on $\mathring{V}$, $\mathring{\boldsymbol{\mathcal{P}}}_N(\mathring{V}) = \{\mathring{\boldsymbol{v}} \in \mathcal{P}_N^3 \mid \mathring{\boldsymbol{\nabla}}\cdot\mathring{\boldsymbol{v}} = 0 \text{ in } \mathring{V}, \mathring{\boldsymbol{r}}\cdot\mathring{\boldsymbol{v}} = 0 \text{ on } \partial\mathring{V}\}$. By (3.4) $\mathring{\boldsymbol{\nabla}}\cdot\mathring{\boldsymbol{v}} = \boldsymbol{\nabla}\cdot\boldsymbol{v}$ and $\boldsymbol{n} = \boldsymbol{L}\cdot\mathring{\boldsymbol{r}}$, noting (1.5), and $\boldsymbol{n}\cdot\boldsymbol{v} = \mathring{\boldsymbol{r}}\cdot\mathring{\boldsymbol{v}}$. Thus $\mathring{\boldsymbol{v}} \in \mathring{\boldsymbol{\mathcal{P}}}_N(\mathring{V})$ if and only if $\boldsymbol{v} \in \boldsymbol{\mathcal{P}}_N(V)$.

If $\boldsymbol{v} \in \boldsymbol{\mathcal{P}}_N(V)$ then $\mathring{\boldsymbol{v}} = \boldsymbol{L}\cdot\boldsymbol{v} = \boldsymbol{L}\cdot\boldsymbol{S}\{s\} + \boldsymbol{L}\cdot\boldsymbol{T}\{t\} = \mathring{\boldsymbol{S}}\{s\} + \mathring{\boldsymbol{T}}\{t\}$, where

$$\mathring{\boldsymbol{T}}\{t\} := \mathring{\boldsymbol{\nabla}}\times\{t\mathring{\boldsymbol{r}}\}, \quad \mathring{\boldsymbol{S}}\{s\} := \mathring{\boldsymbol{\nabla}}\times\mathring{\boldsymbol{T}}\{s\mathring{\boldsymbol{r}}\}, \quad \oint t\,\mathrm{d}\Omega = 0, \quad \oint s\,\mathrm{d}\Omega = 0, \tag{3.5a–d}$$

with $t \in \mathring{\mathcal{P}}_N$, $s \in \mathring{\mathcal{P}}_{N+1}$ and $\mathrm{d}\Omega = \sin\theta\,\mathrm{d}\theta\,\mathrm{d}\phi$ is the element of solid angle on the unit sphere in $\mathring{E}^3$. Conversely, $\boldsymbol{v} = \boldsymbol{L}^{-1}\cdot\mathring{\boldsymbol{S}}\{s\} + \boldsymbol{L}^{-1}\cdot\mathring{\boldsymbol{T}}\{t\}$. The component of $\mathring{\boldsymbol{v}}$ in the direction of a constant vector $\boldsymbol{c}$ is $\boldsymbol{c}\cdot\mathring{\boldsymbol{v}} = -(\boldsymbol{c}\cdot\mathring{\boldsymbol{r}})\mathring{\nabla}^2 s + \boldsymbol{c}\cdot\mathring{\boldsymbol{\nabla}}(s + \mathring{\boldsymbol{r}}\cdot\mathring{\boldsymbol{\nabla}}s) - \boldsymbol{c}\times\mathring{\boldsymbol{r}}\cdot\mathring{\boldsymbol{\nabla}}t$. Thus, if $t \in \mathring{\mathcal{P}}_N$ and $s \in \mathring{\mathcal{P}}_{N+1}$, then $\mathring{\boldsymbol{v}} \in \mathring{\mathcal{P}}_N^3$. Conversely, if $\mathring{\boldsymbol{v}} \in \mathcal{P}_N^3$ and $\mathring{\boldsymbol{\nabla}}\cdot\mathring{\boldsymbol{v}} = 0$, then $t \in \mathring{\mathcal{P}}_N$ and $s \in \mathring{\mathcal{P}}_{N+1}$. This follows from the following Lemma 3.1 and the equations $\mathring{\boldsymbol{r}}\cdot\mathring{\boldsymbol{v}} = -\mathring{\Lambda}^2 s$ and $\mathring{\boldsymbol{r}}\cdot\mathring{\boldsymbol{\nabla}}\times\mathring{\boldsymbol{v}} = -\mathring{\Lambda}^2 t$, noting $\oint\mathring{\boldsymbol{r}}\cdot\mathring{\boldsymbol{v}}\,\mathrm{d}\Omega = 0$ since $\mathring{\boldsymbol{\nabla}}\cdot\mathring{\boldsymbol{v}} = 0$.

LEMMA 3.1. *If $f \in \mathring{\mathcal{P}}_n$ with $\oint f\,\mathrm{d}\Omega = 0$ then $\mathring{\Lambda}^{-2} f \in \mathring{\mathcal{P}}_n$.*

*Proof.* The polynomial $f$ has a complex spherical harmonic expansion of the form (see MacRobert 1947, p. 140),

$$f(\mathring{x}, \mathring{y}, \mathring{z}) = \sum_{n=1}^{N}{}' \sum_{p=n}^{N} \sum_{m=-n}^{n} f_{n,p}^m r^p Y_n^m(\theta, \phi), \tag{3.6}$$

where the $f_{n,p}^m$ are constant and the prime on the $p$-sum indicates summation over $p = n, n+2, n+4, \ldots$ . For any spherical harmonic $Y_n^m(\theta, \phi)$ of degree $n \geqslant 1$ and order $m$, $\mathring{\Lambda}^{-2} h(r) Y_n^m = -h(r) Y_n^m/[n(n+1)]$, where $h(r)$ is any radial function and $\mathring{\boldsymbol{\Lambda}} := \mathring{\boldsymbol{r}}\times\mathring{\boldsymbol{\nabla}}$. □

https://doi.org/10.1017/jfm.2017.669 Published online by Cambridge University Press

To construct a polynomial toroidal–poloidal basis of $\mathcal{P}_N(V)$ observe that the potentials $t \in \mathcal{P}_N$ and $s \in \mathcal{P}_{N+1}$ have spherical harmonic expansions of the form (see MacRobert 1947, p. 140)

$$t = \sum_{n=1}^{N} \sum_{m=-n}^{n} \left( \sum_{j=0}^{\lfloor (N-n)/2 \rfloor} t_{n,j}^m r^{2j} \right) r^n Y_n^m(\theta, \phi) \tag{3.7}$$

$$s = \sum_{n=1}^{N+1} \sum_{m=-n}^{n} \left( \sum_{j=0}^{\lfloor (N+1-n)/2 \rfloor} \tilde{s}_{n,j}^m r^{2j} \right) r^n Y_n^m(\theta, \phi), \tag{3.8}$$

noting (3.5). As for a spherical $V$ (Ivers *et al.* 2015) the dimension of the toroidal subspace $\mathcal{P}_N^T$ of $\mathcal{P}_N(V)$ is

$$\dim \mathcal{P}_N^T = \begin{cases} \frac{1}{6}N(N^2+6N+8), & N \text{ even}; \\ \frac{1}{6}(N+1)(N^2+5N+3), & N \text{ odd}. \end{cases} \tag{3.9}$$

The coefficients $\tilde{s}_{n,j}^m$ must be adjusted to satisfy the boundary condition on the poloidal flows: on $r=1$, $s = \sum_{j=0}^{\lfloor (N+1-n)/2 \rfloor} \tilde{s}_{n,j}^m = 0$. Thus $\tilde{s}_{N,0}^m = 0$, $\tilde{s}_{N+1,0}^m = 0$ and elimination of $\tilde{s}_{n,0}^m$, $n = 1 : N-1$ gives

$$s = \sum_{n=1}^{N-1} \sum_{m=-n}^{n} \left( \sum_{j=1}^{\lfloor (N+1-n)/2 \rfloor} \tilde{s}_{n,j}^m (r^{2j} - 1) \right) r^n Y_n^m(\theta, \phi), \tag{3.10}$$

from which it is clear that $1 - r^2 = 1 - (x^2+y^2)/a^2 - z^2/c^2$ is a factor of $s$. Hence

$$s = (1-r^2) \sum_{n=1}^{N-1} \sum_{m=-n}^{n} \left( \sum_{j=0}^{\lfloor (N+1-n)/2 \rfloor - 1} s_{n,j}^m r^{2j} \right) r^n Y_n^m(\theta, \phi), \tag{3.11}$$

where the new coefficients $s_{n,j}^m$ are independent. Thus the dimension of the poloidal subspace $\mathcal{P}_N^P$ of $\mathcal{P}_N(V)$ is the same as for a spherical $V$ (Ivers *et al.* 2015),

$$\dim \mathcal{P}_N^P = \begin{cases} \frac{1}{6}N(N^2+3N-1), & N \text{ even}; \\ \frac{1}{6}(N-1)(N+1)(N+3), & N \text{ odd}. \end{cases} \tag{3.12}$$

Finally, combining (3.9) and (3.12) yields $\dim \mathcal{P}_N(V) = \dim \mathcal{P}_N^T(V) + \dim \mathcal{P}_N^P(V) = C_N$, i.e. the dimension of $\mathcal{P}_N(V)$ equals the number of aligned Coriolis velocity modes of degree $N$ or less as in (2.18). If $\mathring{\boldsymbol{t}}_{n,j}^m := \mathring{\boldsymbol{\nabla}} \times \{r^{n+2j} Y_n^m(\theta, \phi)\mathring{\boldsymbol{r}}\}$, then $\{\boldsymbol{t}_{n,j}^m\}$ where $\boldsymbol{t}_{n,j}^m := \boldsymbol{L}^{-1} \cdot \mathring{\boldsymbol{t}}_{n,j}^m$ and $n = 1 : N$, $|m| \leqslant n$, $j = 0 : \lfloor (N-n)/2 \rfloor$ is a basis of $\mathcal{P}_N^T(V)$. Similarly, if $\mathring{\boldsymbol{s}}_{n,j}^m := \mathring{\boldsymbol{\nabla}} \times \mathring{\boldsymbol{\nabla}} \times \{(1-r^2) r^{n+2j} Y_n^m(\theta, \phi)\mathring{\boldsymbol{r}}\}$, then $\{\boldsymbol{s}_{n,j}^m\}$ where $\boldsymbol{s}_{n,j}^m := \boldsymbol{L}^{-1} \cdot \mathring{\boldsymbol{s}}_{n,j}^m$ and $n = 1 : N-1$, $|m| \leqslant n$, $j = 0 : \lfloor (N+1-n)/2 \rfloor - 1$ is a basis of $\mathcal{P}_N^P(V)$.

Any basis of $\mathcal{P}_1(V)$ is purely toroidal and consists of linear combinations of the three modes $\{\boldsymbol{t}_{1,0}^0, \boldsymbol{t}_{1,0}^{\pm 1}\}$; a (tilted) Coriolis mode basis is constructed in the following subsection. Any basis of $\mathcal{P}_2(V)$ is mixed toroidal–poloidal and consists of linear combinations of the 11 modes $\{\boldsymbol{t}_{1,0}^0, \boldsymbol{t}_{1,0}^{\pm 1}, \boldsymbol{t}_{2,0}^0, \boldsymbol{t}_{2,0}^{\pm 1}, \boldsymbol{t}_{2,0}^{\pm 2}, \boldsymbol{s}_{1,0}^0, \boldsymbol{s}_{1,0}^{\pm 1}\}$. Any linear combination of the poloidal flows $\{\boldsymbol{s}_{1,0}^0, \boldsymbol{s}_{1,0}^{\pm 1}\}$ has a poloidal potential of the form $s = (1/2)(1-r^2)\boldsymbol{s} \cdot \mathring{\boldsymbol{r}}$ where $\boldsymbol{s}$ is a constant vector. The associated poloidal flow is $\mathring{\boldsymbol{S}}\{(1/2)(1-r^2)\boldsymbol{s} \cdot \mathring{\boldsymbol{r}}\} = (1-2r^2)\boldsymbol{s} + \boldsymbol{s} \cdot \mathring{\boldsymbol{r}}\mathring{\boldsymbol{r}}$.

https://doi.org/10.1017/jfm.2017.669 Published online by Cambridge University Press

### 3.2. *The linear Coriolis velocity modes*

The only Coriolis modes for $N=1$ are toroidal, since they must be linear combinations of $\{\boldsymbol{t}^0_{1,0}, \boldsymbol{t}^{\pm1}_{1,0}\}$. This property can be used to explicitly construct them. It is shown in § 5.2 that these are the only modes with non-zero angular momentum. The $N=1$ aligned modes have been explicitly constructed by Vantieghem (2014) in the tri-axial ellipsoid case. If $N=1$, the toroidal potential is of the form $t=\boldsymbol{t}\cdot\mathring{\boldsymbol{r}}$, where $\boldsymbol{t}$ is a constant vector, the scaled velocity $\mathring{\boldsymbol{v}}=\mathring{\boldsymbol{T}}\{\boldsymbol{t}\cdot\mathring{\boldsymbol{r}}\}=\mathring{\boldsymbol{\nabla}}t\times\mathring{\boldsymbol{r}}=\boldsymbol{t}\times\mathring{\boldsymbol{r}}$ and the physical velocity

$$\boldsymbol{v}=\boldsymbol{L}^{-1}\cdot\mathring{\boldsymbol{v}}=\boldsymbol{L}^{-1}\cdot\boldsymbol{t}\times\mathring{\boldsymbol{r}}=\boldsymbol{L}^{-1}\cdot\boldsymbol{t}\times\boldsymbol{L}\cdot\boldsymbol{r}. \tag{3.13}$$

(Cross-products are evaluated before dot products.) In matrix form

$$\boldsymbol{L}^{-1}\cdot\boldsymbol{t}\times\boldsymbol{L}=\begin{pmatrix}0 & -t_z & t_ya/c\\ t_z & 0 & -t_xa/c\\ -t_yc/a & t_xc/a & 0\end{pmatrix} \tag{3.14}$$

and thus

$$\boldsymbol{v}=(t_yza/c-t_zy)\boldsymbol{i}+(t_zx-t_xza/c)\boldsymbol{j}+(t_xy-t_yx)c/a\boldsymbol{k}. \tag{3.15}$$

If $\boldsymbol{t}$ is real, then $(\boldsymbol{t}\cdot\boldsymbol{L})\cdot\boldsymbol{v}=\boldsymbol{t}\cdot\boldsymbol{t}\times\boldsymbol{L}\cdot\boldsymbol{r}=0$; otherwise $(\mathrm{Re}\,\boldsymbol{t}\cdot\boldsymbol{L})\cdot\mathrm{Re}\,\boldsymbol{v}=0$ and $(\mathrm{Im}\,\boldsymbol{t}\cdot\boldsymbol{L})\cdot\mathrm{Im}\,\boldsymbol{v}=0$. Thus $\boldsymbol{v}$, or $\mathrm{Re}\,\boldsymbol{v}$ and $\mathrm{Im}\,\boldsymbol{v}$ if $\boldsymbol{v}$ is complex, are planar flows in planes perpendicular to $\boldsymbol{t}\cdot\boldsymbol{L}$, $\mathrm{Re}\,\boldsymbol{t}\cdot\boldsymbol{L}$ or $\mathrm{Im}\,\boldsymbol{t}\cdot\boldsymbol{L}$. The pressure $p=(1/2)\boldsymbol{r}\cdot\boldsymbol{P}\cdot\boldsymbol{r}+\boldsymbol{q}\cdot\boldsymbol{r}$, where $\boldsymbol{P}$ is a constant symmetric matrix and $\boldsymbol{q}$ is a constant vector. Thus $\boldsymbol{\nabla}p=\boldsymbol{P}\cdot\boldsymbol{r}+\boldsymbol{q}$ and

$$\mathcal{C}\boldsymbol{v}=\widehat{\boldsymbol{\Omega}}\times\boldsymbol{L}^{-1}\cdot\boldsymbol{t}\times\boldsymbol{L}\cdot\boldsymbol{r}+\boldsymbol{P}\cdot\boldsymbol{r}+\boldsymbol{q}=\lambda\boldsymbol{L}^{-1}\cdot\boldsymbol{t}\times\boldsymbol{L}\cdot\boldsymbol{r} \tag{3.16}$$

for all $\boldsymbol{r}$, which implies $\boldsymbol{q}=\boldsymbol{0}$ and

$$\widehat{\boldsymbol{\Omega}}\times\boldsymbol{L}^{-1}\cdot(\boldsymbol{t}\times\boldsymbol{L})+\boldsymbol{P}=\lambda\boldsymbol{L}^{-1}\cdot(\boldsymbol{t}\times\boldsymbol{L}), \tag{3.17}$$

where

$$\widehat{\boldsymbol{\Omega}}\times\boldsymbol{L}^{-1}\cdot\boldsymbol{t}\times\boldsymbol{L}=\begin{pmatrix}-(\beta t_yc/a+\gamma t_z) & \beta t_xc/a & \gamma t_xa/c\\ \alpha t_yc/a & -(\alpha t_xc/a+\gamma t_z) & \gamma t_ya/c\\ \alpha t_z & \beta t_z & -(\alpha t_x+\beta t_y)a/c\end{pmatrix}. \tag{3.18}$$

Equation (3.17) yields the three equations

$$P_{11}=\beta t_yc/a+\gamma t_z,\quad P_{22}=\alpha t_xc/a+\gamma t_z,\quad P_{33}=(\alpha t_x+\beta t_y)a/c, \tag{3.19a–c}$$

which determine $P_{11}$, $P_{22}$, $P_{33}$ if $\boldsymbol{t}$ and $\lambda$ are known, and the six equations

$$\left.\begin{aligned}\beta t_xc/a+P_{12}=-\lambda t_z,\quad \gamma t_ya/c+P_{23}=-\lambda t_xa/c,\quad \alpha t_z+P_{31}=-\lambda t_yc/a,\\ \alpha t_yc/a+P_{21}=\lambda t_z,\quad \beta t_z+P_{32}=\lambda t_xc/a,\quad \gamma t_xa/c+P_{13}=\lambda t_ya/c,\end{aligned}\right\} \tag{3.20}$$

which determine $P_{ij}$ if $i\neq j$, $\lambda$ and $\boldsymbol{t}$. Using the symmetry of $\boldsymbol{P}$ to eliminate $\lambda$ gives

$$\left.\begin{aligned}P_{12}=P_{21}=-\frac{1}{2}(\beta t_x+\alpha t_y)c/a,\quad P_{23}=P_{32}=-\frac{\gamma t_y+\beta t_za/c}{a/c+c/a},\\ P_{13}=P_{31}=-\frac{\gamma t_x+\alpha t_za/c}{a/c+c/a},\end{aligned}\right\} \tag{3.21}$$

https://doi.org/10.1017/jfm.2017.669 Published online by Cambridge University Press

and to eliminate the $P_{ij}$ yields the generalised eigenproblem,

$$\begin{pmatrix} \lambda(a/c+c/a) & \gamma a/c & -\beta \\ -\gamma a/c & \lambda(a/c+c/a) & \alpha \\ \beta & -\alpha & \lambda 2a/c \end{pmatrix} \begin{pmatrix} t_x \\ t_y \\ t_z \end{pmatrix} = \boldsymbol{0}. \tag{3.22}$$

The eigenvalues are purely imaginary since the eigenproblem is skew symmetric with a symmetric positive definite weight matrix. Solutions with $\boldsymbol{t} \neq \boldsymbol{0}$ exist if and only if $\lambda$ satisfies

$$\begin{vmatrix} \lambda(a/c+c/a) & \gamma a/c & -\beta \\ -\gamma a/c & \lambda(a/c+c/a) & \alpha \\ \beta & -\alpha & 2\lambda a/c \end{vmatrix} = 0. \tag{3.23}$$

For a spheroid the $x$-axis can be chosen so that $\boldsymbol{\Omega}$ lies in the $xz$-plane, i.e. $\alpha = \sin\Theta$, $\beta = 0$, $\gamma = \cos\Theta$, so the frequencies are given by $\omega = 0, \pm\omega_1$ where

$$\omega_1 = \frac{\sqrt{\frac{1}{2}\alpha^2(1+c^2/a^2)c^2/a^2 + \gamma^2}}{1+c^2/a^2}, \quad 0 < \omega_1 < 1. \tag{3.24}$$

This formula agrees with Vantieghem (2014) if the rotation is aligned with a principal axis, i.e. $\Theta = 0$, $\pi$ (symmetry aligned rotation) or $\Theta = \pi/2$. Thus there exists a geostrophic mode of degree $N = 1$ for any tilt angle $\Theta$, and the frequencies satisfy $|\omega| < 1$, which is consistent with Theorem 1.1(f). All geostrophic modes are constructed in § 5.1. The eigenvectors $\boldsymbol{t}$ are

$$\boldsymbol{t}_{1,0} = T_{1,0} \begin{pmatrix} \alpha c/a \\ 0 \\ \gamma \end{pmatrix}, \quad \boldsymbol{t}_{1,\pm\omega_1} = T_{1,\pm\omega_1} \begin{pmatrix} -\gamma/(1+c^2/a^2) \\ \pm \mathrm{i}\omega_1 \\ \frac{1}{2}\alpha c/a \end{pmatrix}, \tag{3.25a,b}$$

where $T_{1,0}$ and $T_{1,\pm\omega_1}$ are normalisation constants.

Since $(\boldsymbol{L}^{-1}\cdot\boldsymbol{t}_1 \times \mathring{\boldsymbol{r}})\cdot(\boldsymbol{L}^{-1}\cdot\boldsymbol{t}_2^* \times \mathring{\boldsymbol{r}}) = -\mathring{\boldsymbol{r}}\cdot(\boldsymbol{t}_1 \times \boldsymbol{D}^{-1} \times \boldsymbol{t}_2^*)\cdot\mathring{\boldsymbol{r}}$ where $\boldsymbol{D} := \boldsymbol{L}\cdot\boldsymbol{L}$ and the asterisk denotes the complex conjugate,

$$(\boldsymbol{v}_1, \boldsymbol{v}_2) = -\int_V \mathring{\boldsymbol{r}}\cdot(\boldsymbol{t}_1 \times \boldsymbol{D}^{-1} \times \boldsymbol{t}_2^*)\cdot\mathring{\boldsymbol{r}} a^2 c \,\mathrm{d}\mathring{V} = -\frac{1}{5}|V|\,\mathrm{tr}(\boldsymbol{t}_1 \times \boldsymbol{D}^{-1} \times \boldsymbol{t}_2^*), \tag{3.26}$$

where $\mathrm{d}V = a^2 c\,\mathrm{d}\mathring{V}$ and $|V| = 4\pi a^2 c/3$ is the volume of $V$. In Cartesian matrix form

$$\boldsymbol{t}_1 \times \boldsymbol{D}^{-1} \times \boldsymbol{t}_2^* = \begin{pmatrix} -c^2 t_{1y} t_{2y}^* - a^2 t_{1z} t_{2z}^* & c^2 t_{1y} t_{2x}^* & a^2 t_{1z} t_{2x}^* \\ c^2 t_{1x} t_{2y}^* & -c^2 t_{1x} t_{2x}^* - a^2 t_{1z} t_{2z}^* & a^2 t_{1z} t_{2y}^* \\ a^2 t_{1x} t_{2z}^* & a^2 t_{1y} t_{2z}^* & -a^2 t_{1x} t_{2x}^* - a^2 t_{1y} t_{2y}^* \end{pmatrix}, \tag{3.27}$$

thus $(\boldsymbol{v}_1, \boldsymbol{v}_2) = (1/5)|V|\{(a^2+c^2)(t_{1x}t_{2x}^* + t_{1y}t_{2y}^*) + 2a^2 t_{1z}t_{2z}^*\}$. Hence the $N = 1$ modes are orthogonal, $(\boldsymbol{v}_{1,0}, \boldsymbol{v}_{1,\pm\omega_1}) = 0$ and $(\boldsymbol{v}_{1,\omega_1}, \boldsymbol{v}_{1,-\omega_1}) = 0$ and the norm is given by $\|\boldsymbol{v}\|^2 = (1/5)|V|\{(a^2+c^2)(|t_x|^2 + |t_y|^2) + 2a^2|t_z|^2\}$, which gives

$$T_{1,0}^{-1} = \sqrt{\tfrac{2}{5}|V|}a\omega_1(1+c^2/a^2), \quad T_{1,\omega_1} = T_{1,-\omega_1} = T_{1,0}\sqrt{1+c^2/a^2}. \tag{3.28a,b}$$

https://doi.org/10.1017/jfm.2017.669 Published online by Cambridge University Press

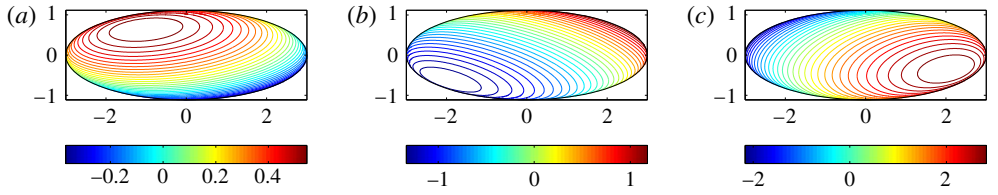



FIGURE 3. (Colour online) Orthographic projections of the streamlines of the linear velocity spatial modes (i.e. the level contours of the toroidal potentials), $\boldsymbol{v}_{1,0}$, $\mathrm{Re}\,\boldsymbol{v}_{1,\omega_1}$ and $\mathrm{Im}\,\boldsymbol{v}_{1,\omega_1}$ (left to right), on the boundary for $a=3$, $c=1$, $\Theta=\pi/3$ viewed from co-latitude $4\pi/9$, longitude $\pi/4$.

The choice of phase ensures $\boldsymbol{t}^*_{1,-\omega_1}=\boldsymbol{t}_{1,\omega_1}$, $\mathring{\boldsymbol{v}}^*_{1,-\omega_1}=\mathring{\boldsymbol{v}}_{1,\omega_1}$ and $\boldsymbol{v}^*_{1,-\omega_1}=\boldsymbol{v}_{1,\omega_1}$, where the velocity modes, $\mathring{\boldsymbol{v}}_{1,0}=\boldsymbol{t}_{1,0}\times\mathring{\boldsymbol{r}}$, $\mathring{\boldsymbol{v}}_{1,\pm\omega_1}=\boldsymbol{t}_{1,\pm\omega_1}\times\mathring{\boldsymbol{r}}$ and by (3.15),

$$\boldsymbol{v}_{1,0}=T_{1,0}\left\{\gamma(\boldsymbol{j}x-\boldsymbol{i}y)-\frac{\alpha c}{a}\left(\boldsymbol{j}\frac{za}{c}-\boldsymbol{k}\frac{yc}{a}\right)\right\} \tag{3.29}$$

$$\boldsymbol{v}_{1,\pm\omega_1}=T_{1,\omega_1}\left\{\frac{\gamma}{1+c^2/a^2}\left(\boldsymbol{j}\frac{za}{c}-\boldsymbol{k}\frac{yc}{a}\right)+\frac{1}{2}\frac{\alpha c}{a}(\boldsymbol{j}x-\boldsymbol{i}y)\pm\mathrm{i}\omega_1\left(\boldsymbol{i}\frac{za}{c}-\boldsymbol{k}\frac{xc}{a}\right)\right\}. \tag{3.30}$$

As $\alpha\to 0$, $\gamma\to 1$ and $\boldsymbol{v}_{1,0}\to\boldsymbol{k}\times\boldsymbol{\Omega}$. From the remark following (3.15) the flows $\boldsymbol{v}_{1,0}$, $\mathrm{Re}\,\boldsymbol{v}_{1,\omega_1}=\mathrm{Re}\,\boldsymbol{v}_{1,-\omega_1}$ and $\mathrm{Im}\,\boldsymbol{v}_{1,\omega_1}=-\mathrm{Im}\,\boldsymbol{v}_{1,-\omega_1}$ lie in planes normal to $\boldsymbol{N}=\alpha/a^2\boldsymbol{i}+\gamma/c^2\boldsymbol{k}$, $\boldsymbol{N}_r=-\gamma/(1+c^2/a^2)\boldsymbol{i}+(1/2)\alpha\boldsymbol{k}$ and $\boldsymbol{N}_i=\boldsymbol{j}$. See figure 3.

$$P_{1,0}=\tfrac{1}{2}T_{1,0}(\gamma x-\alpha z)^2+\tfrac{1}{2}T_{1,0}[\alpha^2(c/a)^2+\gamma^2]y^2. \tag{3.31}$$

$$\begin{aligned}P_{1,\pm\omega_1}\;=\;&T_{1,\omega_1}\left\{\frac{1}{4}\alpha\gamma(x^2+y^2)c/a-\frac{1}{2}\alpha\gamma\frac{(y^2c/a+z^2a/c)}{(1+c^2/a^2)}+\left(\frac{\gamma^2}{1+c^2/a^2}-\omega_1^2\right)xza/c\right\}\\&\mp\mathrm{i}\omega_1T_{1,\omega_1}\left(\frac{1}{2}\alpha xyc/a+\frac{\gamma yz}{a/c+c/a}\right).\end{aligned} \tag{3.32}$$

## 4. The Coriolis operator on polynomial flows in a spheroid

If the Coriolis operator $\mathcal{C}$ is restricted to act on polynomial flows $\mathcal{P}_N(V)$ of degree $N$ or less where $V$ is a sphere then $\mathcal{C}:\mathcal{P}_N(V)\to\mathcal{P}_N(V)$, i.e. the restricted Coriolis operator $\mathcal{C}:\mathcal{P}_N(V)\to\mathcal{P}_N(V)$ is well defined and maps polynomial flows to polynomial flows of the same degree (Ivers *et al.* 2015). It is also true if $V$ is a spheroid but not for general $V$. This is Theorem 4.3, the essential result of the paper, and follows from Theorem 4.2, which is the fundamental tool.

THEOREM 4.1 (Polynomial Laplace–Neumann problem in a spheroid). *There exists a unique solution $\varphi$ of Laplace's equation $\nabla^2\varphi=0$ in the spheroid $V$, subject to $\boldsymbol{n}\cdot\nabla\varphi=q$ on $\partial V$, where the normal $\boldsymbol{n}:=(x\boldsymbol{i}+y\boldsymbol{j})/a^2+z\boldsymbol{k}/c^2$ and $q\in\mathcal{P}_{N_1}$, and to the consistency and uniqueness conditions,*

$$\int_{\partial V}\frac{q}{|\boldsymbol{n}|}\,\mathrm{d}S=0,\qquad\int_{\partial V}\frac{\varphi}{|\boldsymbol{n}|}\,\mathrm{d}S=0, \tag{4.1a,b}$$

*respectively, and moreover, $\varphi\in\mathcal{P}_{N_1}$.*

https://doi.org/10.1017/jfm.2017.669 Published online by Cambridge University Press

*Proof.* The consistency condition (4.1) is necessary, since

$$0=\int_V \nabla^2\varphi\,\mathrm{d}V=\int_{\partial V}\boldsymbol{\nabla}\varphi\cdot\mathrm{d}\boldsymbol{S}=0=\int_{\partial V}\frac{q}{|\boldsymbol{n}|}\,\mathrm{d}S. \tag{4.2}$$

The oblate and prolate cases are treated separately. Consider the oblate case $a>c$ and introduce orthogonal confocal oblate ($a\geqslant c$) spheroidal coordinates $(\eta,\phi,\xi)$,

$$s=\mathrm{d}\sqrt{1+\eta^2}\sqrt{1-\xi^2},\quad z=\mathrm{d}\eta\xi,\quad d:=\sqrt{a^2-c^2}. \tag{4.3a–c}$$

Other commonly used confocal oblate spheroidal coordinates are related to $(\eta,\phi,\xi)$ by simple changes of variables, including $\eta=\sinh\eta_1$, $\eta=\sqrt{\eta_2^2-1}$, $\eta=\eta_3/d$ and $\xi=\cos\theta$. The element of arc length is

$$\mathrm{d}\ell^2=d^2\left(\frac{\xi^2+\eta^2}{1+\eta^2}\mathrm{d}\eta^2+(1-\xi^2)(1+\eta^2)\,\mathrm{d}\phi^2+\frac{\xi^2+\eta^2}{1-\xi^2}\,\mathrm{d}\xi^2\right), \tag{4.4}$$

the scale factors are

$$h_\eta=d\sqrt{\frac{\xi^2+\eta^2}{1+\eta^2}},\quad h_\phi=d\sqrt{1+\eta^2}\sqrt{1-\xi^2}=s,\quad h_\xi=d\sqrt{\frac{\xi^2+\eta^2}{1-\xi^2}} \tag{4.5a–c}$$

and the unit basis vector

$$\boldsymbol{1}_\eta=h_\eta^{-1}\partial_\eta\boldsymbol{r}=h_\eta^{-1}\partial_\eta(s\boldsymbol{1}_s+z\boldsymbol{1}_z)=\sqrt{\frac{1-\xi^2}{\xi^2+\eta^2}}\eta\boldsymbol{1}_s+\sqrt{\frac{1+\eta^2}{\xi^2+\eta^2}}\xi\boldsymbol{1}_z. \tag{4.6}$$

The boundary $\partial V$ is parametrised by $s=a\sin\theta$ and $z=c\cos\theta$, i.e. the $\eta$-surface with $\eta=c/d$ and $\xi=\cos\theta$, $0\leqslant\theta\leqslant\pi$. On $\partial V$ the scale factors are $h_\eta=d\sqrt{c^2+d^2\cos^2\theta}/a$, $h_\phi=a\sin\theta$, $h_\xi=\sqrt{c^2+d^2\cos^2\theta}/\sin\theta$ and the basis vector

$$\boldsymbol{1}_\eta=(c\sin\theta\boldsymbol{1}_s+a\cos\theta\boldsymbol{1}_z)/\sqrt{c^2+d^2\cos^2\theta} \tag{4.7}$$

is the unit normal. On $\partial V$ the vector field $\boldsymbol{n}=\boldsymbol{1}_s s/a^2+\boldsymbol{1}_z z/c^2$ reduces to $\boldsymbol{n}=\boldsymbol{1}_s\sin\theta/a+\boldsymbol{1}_z\cos\theta/c$ and $|\boldsymbol{n}|=\sqrt{c^2+d^2\cos^2\theta}/ac=h_\eta/cd$. In general, $\boldsymbol{n}\nparallel\boldsymbol{1}_\eta$, except on $\partial V$, where $\boldsymbol{n}=|\boldsymbol{n}|\boldsymbol{1}_\eta$, and its principal axes, and hence $\boldsymbol{n}\cdot\boldsymbol{\nabla}=(cd)^{-1}\partial_\eta$. The element of surface area on $\partial V$ is $\mathrm{d}S=h_\xi h_\phi\,\mathrm{d}\xi\,\mathrm{d}\phi=a\sqrt{c^2+d^2\cos^2\theta}\sin\theta\,\mathrm{d}\theta\,\mathrm{d}\phi$, thus $\mathrm{d}S/|\boldsymbol{n}|=a^2c\sin\theta\,\mathrm{d}\theta\,\mathrm{d}\phi$.

The Laplacian is given in oblate spheroidal coordinates by

$$d^2(\xi^2+\eta^2)\nabla^2u=\partial_\eta(1+\eta^2)\partial_\eta u+\partial_\xi(1-\xi^2)\partial_\xi u+[(1-\xi^2)^{-1}-(1+\eta^2)^{-1}]\partial_{\phi\phi}u. \tag{4.8}$$

The interior harmonic solutions are of the form $u=P_n^m(\mathrm{i}\eta)P_n^m(\xi)\mathrm{e}^{\mathrm{i}m\phi}$ and hence the general interior solution is

$$\varphi=\sum_{n=0}^{\infty}\sum_{m=-n}^{n}\varphi_n^m P_n^m(\xi)P_n^m(\mathrm{i}\eta)\mathrm{e}^{\mathrm{i}m\phi}, \tag{4.9}$$

where the $\varphi_n^m$ are constants.

https://doi.org/10.1017/jfm.2017.669 Published online by Cambridge University Press

To impose the Neumann boundary condition on the solution (4.9) it is first shown that a polynomial $q$ in $E^3$ of degree $N_1$ can expanded on $\partial V$ as a linear combination of associated Legendre functions $P_n^m(\xi)$ of degree $N_1$ or less. Let $w := x + \mathrm{i}y$. Then $x = (w + w^*)/2$ and $y = (w - w^*)/2\mathrm{i}$. Since $q \in \mathcal{P}_{N_1}$ it can be written as

$$q(x, y, z) = q((w + w^*)/2, (w - w^*)/2\mathrm{i}, z) = \sum_{j+k+l \leqslant N_1} q_{jkl} w^j (w^*)^k z^l = \sum_{j+k \leqslant N_1} w^j (w^*)^k q_{j,k}(z), \tag{4.10}$$

where the $q_{jkl}$ are constants and $q_{j,k}(z) := \sum_{l=0}^{N_1-(j+k)} q_{jkl} z^l$ is a polynomial in $z$ of degree $N_1 - (j + k)$. But

$$w^j (w^*)^k = \begin{cases} s^{2k}(x + \mathrm{i}y)^{j-k}, & \text{if } j \geqslant k; \\ s^{2j}(x - \mathrm{i}y)^{k-j}, & \text{if } k \geqslant j. \end{cases} \tag{4.11}$$

In either case $w^j (w^*)^k = s^{2\,min(j,k)} s^{|j-k|} \mathrm{e}^{\mathrm{i}(j-k)\phi}$ and hence

$$q(x, y, z) = \sum_{j+k \leqslant N_1} s^{|j-k|} \mathrm{e}^{\mathrm{i}(j-k)\phi} s^{2\,min(j,k)} q_{j,k}(z). \tag{4.12}$$

Let $m = j - k$ and $l = j + k$. Then $2\min(j, k) = (j + k) - |j - k| = l - |m|$, $l - |m|$ must be even and

$$q(x, y, z) = \sum_{l=0}^{N_1}{}' \sum_{m=-l}^{l} s^{|m|} \mathrm{e}^{\mathrm{i}m\phi} s^{l-|m|} q_{N_1-l}^m(z), \tag{4.13}$$

relabelling $q_{j,k}(z)$ as $q_{N_1-l}^m(z)$ using $l, m$ to replace $j, k$. The degree of $q_{N_1-l}^m(z)$ is $N_1 - l$. The prime on the summation indicates that $l - |m|$ is even. On $s = a \sin\theta$, $z = c \cos\theta$

$$q = \sum_{l=0}^{N_1}{}' \sum_{m=-l}^{l} a^l \sin^{|m|}\theta (1 - \cos^2\theta)^{(l-|m|)/2} q_{N_1-l}^m(c\cos\theta) \mathrm{e}^{\mathrm{i}m\phi}. \tag{4.14}$$

The factor $(1 - \cos^2\theta)^{(l-|m|)/2} q_{N_1-l}^m(c\cos\theta)$ is a polynomial of degree $N_1 - |m|$ in $\cos\theta$. Thus $q$ is of the form

$$q = \sum_{l=1}^{N_1} \sum_{m=-l}^{l} q_l^m P_l^m(\cos\theta) \mathrm{e}^{\mathrm{i}m\phi}, \tag{4.15}$$

where the $q_l^m$ are constants and $q_0^0 = 0$ by the consistency condition (4.1*a*).

The boundary condition $\boldsymbol{n} \cdot \nabla\varphi = q$ reduces to $q = |\boldsymbol{n}| \mathbf{1}_\eta \cdot \nabla\varphi = |\boldsymbol{n}| h_\eta^{-1} \partial_\eta \varphi = \partial_\eta \varphi / cd$. Thus on $\partial V$, noting the uniqueness condition (4.1*b*),

$$cd\boldsymbol{n} \cdot \nabla\varphi = \mathrm{i} \sum_{n=1}^{\infty} \sum_{m=-n}^{n} \varphi_n^m P_n^{m\prime}(\mathrm{i}c/d) P_n^m(\cos\theta) \mathrm{e}^{\mathrm{i}m\phi} = cd \sum_{l=1}^{N_1} \sum_{m=-l}^{l} q_l^m P_l^m(\cos\theta) \mathrm{e}^{\mathrm{i}m\phi}. \tag{4.16}$$

Hence

$$\varphi_n^m = \begin{cases} -\dfrac{\mathrm{i}cdq_l^m}{P_n^{m\prime}(\mathrm{i}c/d)}, & \text{if } 1 \leqslant n \leqslant N_1; \\ 0, & \text{otherwise.} \end{cases} \tag{4.17}$$

By the following Lemma 4.1 the derivative of $P_n^m$ has no non-zero imaginary zeros, thus $P_n^{m\prime}(\mathrm{i}c/d) \neq 0$, $\varphi_n^m$ is well defined and the solution $\varphi$ is a unique polynomial of degree $N_1$.

https://doi.org/10.1017/jfm.2017.669 Published online by Cambridge University Press

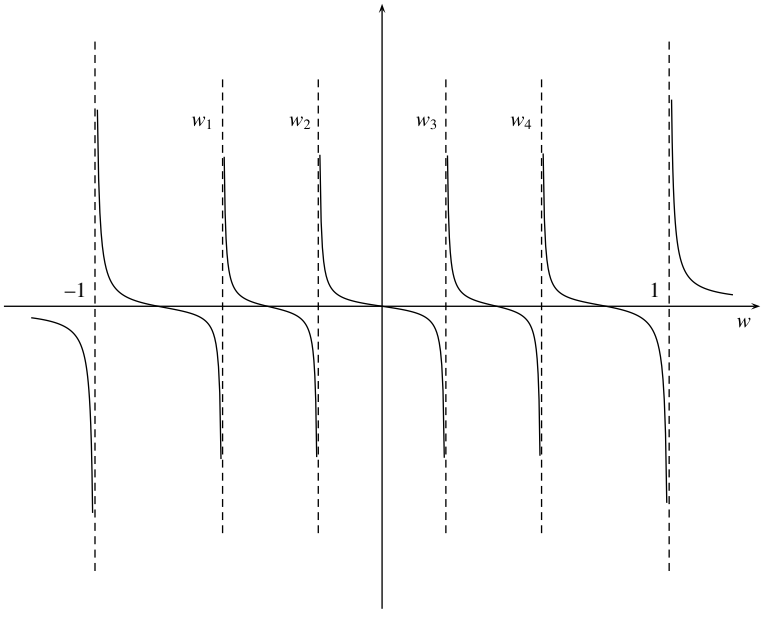



FIGURE 4. A schematic plot of (4.18) showing the five zeros of $\mathrm{d}P_n^m(w)/\mathrm{d}w$, excluding the zeros of $P_n^m(w)$, for $n-|m|=4$.

LEMMA 4.1. *The zeros of the derivative* $\mathrm{d}P_n^m(w)/\mathrm{d}w$ *in the complex* $w$*-plane are real and lie in the interval* $[-1, 1]$.

*Proof.* If $w$ is a zero of $\mathrm{d}P_n^m/\mathrm{d}w$ but not $P_n^m$, then from (2.14) with $\mathring{\omega}$ replaced by $w$ and $\mathring{\omega}_k$ by $w_k$,

$$\frac{1}{P_n^m(w)}\frac{\mathrm{d}P_n^m(w)}{\mathrm{d}w}=\frac{\frac{1}{2}|m|}{w+1}+\frac{\frac{1}{2}|m|}{w-1}+\sum_{k=1}^{n-|m|}\frac{1}{w-w_k}=0. \tag{4.18}$$

Thus $w$ is a zero of the following polynomial of degree $n-|m|+1$,

$$|m|w\prod_{l=1}^{n-|m|}(w-w_l)+(w^2-1)\sum_{k=1}^{n-|m|}\prod_{l=1,l\neq k}^{n-|m|}(w-w_l)=0, \tag{4.19}$$

so there are at most $n-|m|+1$ such zeros. It is easily seen that there are in fact $n-|m|+1$ such zeros, since $w_k\in(-1,1)$ for $k=1:n-|m|$, and these zeros are real and lie in the interval $(-1, 1)$; see figure 4. Since the zeros of $P_n^m(w)$ lie in $[-1, 1]$, the zeros of $\mathrm{d}P_n^m/\mathrm{d}w$ lie in $[-1, 1]$. □

Now consider the prolate case $a<c$ and introduce orthogonal confocal prolate spheroidal coordinates,

$$s=d\sqrt{\eta^2-1}\sqrt{1-\xi^2},\quad z=\mathrm{d}\eta\xi,\quad d=\sqrt{c^2-a^2}. \tag{4.20a–c}$$

Other confocal prolate spheroidal coordinates are related to $(\eta, \phi, \xi)$ by changes of variables. The element of arc length is

$$\mathrm{d}\ell^2=d^2\left(\frac{\eta^2-\xi^2}{\eta^2-1}\,\mathrm{d}\eta^2+(\eta^2-1)(1-\xi^2)\,\mathrm{d}\phi^2+\frac{\eta^2-\xi^2}{1-\xi^2}\,\mathrm{d}\xi^2\right), \tag{4.21}$$

https://doi.org/10.1017/jfm.2017.669 Published online by Cambridge University Press

the scale factors are

$$h_\eta = d\sqrt{\frac{\eta^2-\xi^2}{\eta^2-1}}, \quad h_\phi = d\sqrt{\eta^2-1}\sqrt{1-\xi^2} = s, \quad h_\xi = d\sqrt{\frac{\eta^2-\xi^2}{1-\xi^2}} \qquad (4.22a\text{–}c)$$

and the unit basis vector

$$\mathbf{1}_\eta = h_\eta^{-1}\partial_\eta \boldsymbol{r} = \sqrt{\frac{1-\xi^2}{\eta^2-\xi^2}}\eta\mathbf{1}_s + \sqrt{\frac{\eta^2-1}{\eta^2-\xi^2}}\xi\mathbf{1}_z. \qquad (4.23)$$

The boundary $\partial V$ is parametrised by $s = a\sin\theta$ and $z = c\cos\theta$, i.e. the $\eta$-surface with $\eta = c/d$ and $\xi = \cos\theta$, $0 \leqslant \theta \leqslant \pi$. On $\partial V$ the scale factors are $h_\eta = d\sqrt{c^2 - d^2\cos^2\theta}/a$, $h_\phi = a\sin\theta$, $h_\xi = \sqrt{c^2 - d^2\cos^2\theta}/\sin\theta$, $\boldsymbol{n} = |\boldsymbol{n}|\mathbf{1}_\eta$, $\boldsymbol{n}\cdot\boldsymbol{\nabla} = (cd)^{-1}\partial_\eta$, $\mathrm{d}S = h_\xi h_\phi\,\mathrm{d}\xi\,\mathrm{d}\phi = a\sqrt{c^2 - d^2\cos^2\theta}\,\sin\theta\,\mathrm{d}\theta\,\mathrm{d}\phi$ and $\mathrm{d}S/|\boldsymbol{n}| = a^2 c\,\sin\theta\,\mathrm{d}\theta\,\mathrm{d}\phi$, since $|\boldsymbol{n}| = \sqrt{c^2 - d^2\cos^2\theta}/ac = h_\eta/cd$. In general, $\boldsymbol{n} \nparallel \mathbf{1}_\eta$, except on $\partial V$ or its principal axes.

The Laplacian has the form

$$d^2(\eta^2-\xi^2)\nabla^2 u = \partial_\eta(\eta^2-1)\partial_\eta u + \partial_\xi(1-\xi^2)\partial_\xi u + [(\eta^2-1)^{-1} + (1-\xi^2)^{-1}]\partial_{\phi\phi}u. \quad (4.24)$$

The interior solutions are of the form $u = P_n^m(\eta)P_n^m(\xi)\mathrm{e}^{\mathrm{i}m\phi}$. Hence

$$\varphi = \sum_{n=0}^{\infty}\sum_{m=-n}^{n}\varphi_n^m P_n^m(\xi)P_n^m(\eta)\mathrm{e}^{\mathrm{i}m\phi}. \qquad (4.25)$$

The boundary condition $\boldsymbol{n}\cdot\boldsymbol{\nabla}\varphi = q$ reduces to $q = |\boldsymbol{n}|\mathbf{1}_\eta\cdot\boldsymbol{\nabla}\varphi = |\boldsymbol{n}|h_\eta^{-1}\partial_\eta\varphi = \partial_\eta\varphi/cd$. Thus on $\partial V$ using (4.15),

$$cd\boldsymbol{n}\cdot\boldsymbol{\nabla}\varphi = \sum_{n=1}^{\infty}\sum_{m=-n}^{n}\varphi_n^m P_n^{m\prime}(c/d)P_n^m(\cos\theta)\mathrm{e}^{\mathrm{i}m\phi} = cd\sum_{l=1}^{N_1}\sum_{m=-l}^{l}q_l^m P_l^m(\cos\theta)\mathrm{e}^{\mathrm{i}m\phi}. \quad (4.26)$$

Hence

$$\varphi_n^m = \begin{cases} \dfrac{cdq_l^m}{P_n^{m\prime}(c/d)}, & \text{if } 1 \leqslant n \leqslant N_1; \\ 0, & \text{otherwise.} \end{cases} \qquad (4.27)$$

Since $c > d$ and the derivative $P_n^{m\prime}$ has no real zeros in $(1, \infty)$, $P_n^{m\prime}(c/d) \neq 0$, $\varphi_n^m$ is well defined and the solution $\varphi$ is a unique polynomial of degree $N_1$. □

The following lemma is given in Ivers *et al.* (2015).

LEMMA 4.2 (Polynomial integral of the polynomial Poisson–Neumann problem in $E^3$). *If $f \in \mathcal{P}_{N_2}$, then there exists a solution $\varphi_p$ of Poisson's equation $\nabla^2\varphi = f$ with $\varphi_p \in \mathcal{P}_{N_2+2}$ in $E^3$.*

The fundamental tool of the paper is

https://doi.org/10.1017/jfm.2017.669 Published online by Cambridge University Press

THEOREM 4.2 (Polynomial Poisson–Neumann problem in a spheroid). *If $\varphi$ is a solution of Poisson's equation $\nabla^2\varphi = f$ in the spheroid $V$, $f \in \mathcal{P}_{N_2}$ and $\boldsymbol{n}\cdot\nabla\varphi = q$ on $\partial V$, where $\boldsymbol{n} := (x\mathbf{1}_x + y\mathbf{1}_y)/a + z\mathbf{1}_z/c$, $f$ and $q$ satisfy the consistency condition*

$$\int_V f \,\mathrm{d}V = \int_{\partial V} \frac{q}{|\boldsymbol{n}|}\,\mathrm{d}S \tag{4.28}$$

*and $q \in \mathcal{P}_{N_1}$, subject to the uniqueness condition*

$$\int_{\partial V} \frac{\varphi}{|\boldsymbol{n}|}\,\mathrm{d}S = 0, \tag{4.29}$$

*then $\varphi \in \mathcal{P}_{N_3}$, where $N_3 = \max(N_1, N_2 + 2)$.*

*Proof.* The consistency condition (4.28) is necessary, since

$$\int_V f \,\mathrm{d}V = \int_V \nabla^2\varphi \,\mathrm{d}V = \int_{\partial V} \nabla\varphi\cdot\mathrm{d}\boldsymbol{S} = \int_{\partial V} \frac{q}{|\boldsymbol{n}|}\,\mathrm{d}S. \tag{4.30}$$

By Lemma 4.1 there exists a polynomial $\varphi_p \in \mathcal{P}_{N_2+2}$ such that $\nabla^2\varphi_p = f$ and $\int_{\partial V}\varphi_p/|\boldsymbol{n}|\,\mathrm{d}S = 0$. Thus $\nabla^2(\varphi - \varphi_p) = 0$ in $V$ and $\boldsymbol{n}\cdot\nabla(\varphi - \varphi_p) = q - \boldsymbol{n}\cdot\nabla\varphi_p$ on $\partial V$. Since the consistency conditions of Theorem 4.1 hold, $\int_V(\varphi - \varphi_p)/|\boldsymbol{n}|\,\mathrm{d}V = 0$ and

$$\int_{\partial V}\left(\frac{q}{|\boldsymbol{n}|} - \widehat{\boldsymbol{n}}\cdot\nabla\varphi_p\right)\mathrm{d}S = \int_{\partial V}\frac{q}{|\boldsymbol{n}|}\,\mathrm{d}S - \int_V \nabla^2\varphi_p\,\mathrm{d}V = \int_{\partial V}\frac{q}{|\boldsymbol{n}|}\,\mathrm{d}S - \int_V f\,\mathrm{d}V = 0. \tag{4.31}$$

Theorem 4.1 applies to $\varphi - \varphi_p$ and implies $\varphi - \varphi_p \in \mathcal{P}_{N_1}$. Hence $\varphi \in \mathcal{P}_{N_3}$. □

The essential result of the paper is Theorem 4.3: that $\mathcal{C}$ maps polynomial flows of degree $N$ or less in a spheroid to polynomial flows of degree $N$ or less.

THEOREM 4.3 ($\mathcal{C}$-invariance of polynomial flows in a spheroid). *The space $\mathcal{P}_N(V)$ of polynomial flows of degree $N$ or less on a sphere $V$ is invariant under $\mathcal{C}$, i.e. $\mathcal{C}\mathcal{P}_N(V) \subseteq \mathcal{P}_N(V)$.*

*Proof.* To show the Coriolis operator $\mathcal{C}$ is well defined on $\mathcal{P}_N(V)$ we must show that, if $\boldsymbol{v} \in \mathcal{P}_N(V)$, there exists a pressure $p \in \mathcal{P}_{N+1}$ such that $\mathcal{C}\boldsymbol{v} = \widehat{\boldsymbol{\Omega}}\times\boldsymbol{v} + \nabla p \in \mathcal{P}_N(V)$. We can construct $p$ as in (1.10) so that $\nabla\cdot(\mathcal{C}\boldsymbol{v}) = -\widehat{\boldsymbol{\Omega}}\cdot\nabla\times\boldsymbol{v} + \nabla^2 p = 0$ in $V$ (note the sign correction to Ivers *et al.* 2015) and $\boldsymbol{n}\cdot(\mathcal{C}\boldsymbol{v}) = \boldsymbol{n}\cdot\widehat{\boldsymbol{\Omega}}\times\boldsymbol{v} + \boldsymbol{n}\cdot\nabla p = 0$ on $\partial V$, by Theorem 4.2 with $f = \widehat{\boldsymbol{\Omega}}\cdot\nabla\times\boldsymbol{v} \in \mathcal{P}_{N-1}$ and $q = -\boldsymbol{n}\cdot\widehat{\boldsymbol{\Omega}}\times\boldsymbol{v} \in \mathcal{P}_{N+1}$. Thus $N_1 = N+1$ and $N_2 = N-1$ in that theorem, i.e. $N_3 = N+1$ and hence $p \in \mathcal{P}_{N+1}$. Hence $\mathcal{C}\boldsymbol{v} \in \mathcal{P}_N(V)$. □

It is now shown that the operator $\mathcal{C}$ on $\mathcal{P}_N(V)$ is non-defective, i.e. its eigenvectors span $\mathcal{P}_N(V)$. In fact, $-\mathrm{i}\mathcal{C}$ can be represented by a Hermitian matrix on $\mathcal{P}_N(V)$. The proof is simple on the finite-dimensional space $\mathcal{P}_N(V)$. The result provides a proof of the completeness of the Coriolis modes on the infinite-dimensional space $\boldsymbol{\mathcal{V}}^1(V)$ in Theorem 6.1, without requiring the explicit construction of the modes as a basis of $\mathcal{P}_N(V)$.

https://doi.org/10.1017/jfm.2017.669 Published online by Cambridge University Press

THEOREM 4.4 (Existence and polynomial nature of Coriolis modes in a spheroid). *The finite-dimensional operator $-\mathrm{i}\mathcal{C}$ on $\mathcal{P}_N(V)$ is self-adjoint. The eigenvalues $\lambda = \mathrm{i}\omega$ of $\mathcal{C}$ are purely imaginary and satisfy $|\lambda| = |\omega| < 1$ and the eigenvectors of distinct eigenvalues of $\mathcal{C}$ are orthogonal. The eigenvectors of $\mathcal{C}$ span the finite-dimensional space $\mathcal{P}_N(V)$. The number of Coriolis modes of degree $N$ or less is $C_N$.*

*Proof.* If $\boldsymbol{v}_1, \boldsymbol{v}_2 \in \mathcal{P}_N(V)$, then $(-\mathrm{i}\mathcal{C}\boldsymbol{v}_1, \boldsymbol{v}_2) = (\boldsymbol{v}_1, -\mathrm{i}\mathcal{C}\boldsymbol{v}_2)$ by Theorem 1.1 and $-\mathrm{i}\mathcal{C}$ is self-adjoint since $\mathcal{P}_N(V)$ is finite-dimensional. Thus the eigenvectors of $-\mathrm{i}\mathcal{C}$ span $\mathcal{P}_N(V)$, the eigenvectors of distinct eigenvalues are orthogonal and its eigenvalues are real. If $\boldsymbol{v}$ is an eigenvector of $-\mathrm{i}\mathcal{C}$ corresponding to the eigenvalue $\omega$, then $-\mathrm{i}\mathcal{C}\boldsymbol{v} = \omega\boldsymbol{v}$ and hence $\mathcal{C}\boldsymbol{v} = \lambda\boldsymbol{v}$, i.e. $\boldsymbol{v}$ is an eigenvector of $\mathcal{C}$ corresponding to the eigenvalue $\lambda = \mathrm{i}\omega$. Thus the eigenvectors of $\mathcal{C}$ are complete in the finite-dimensional space $\mathcal{P}_N(V)$ and its eigenvalues are purely imaginary. The bound $|\omega| < 1$ follows as in Theorem 1.1 and the result that $\omega \neq \pm 1$. □

The spaces $\mathcal{P}_N(V)$ are hierarchical in the sense that if $N_1 \leqslant N_2$ and $(\boldsymbol{v}, \omega)$ is an eigenmode of $\mathcal{C}$ in $\mathcal{P}_{N_1}(V)$ then $(\boldsymbol{v}, \omega)$ is an eigenmode of $\mathcal{C}$ in $\mathcal{P}_{N_2}(V)$. Moreover, $(\boldsymbol{v}, \omega)$ is an eigenmode of $\mathcal{C}$ in $\boldsymbol{\mathcal{V}}^1(V)$ and, for any polynomial flow $\boldsymbol{v} \in \mathcal{P}_N(V)$, $(\boldsymbol{v}, \boldsymbol{v}_\alpha) = 0$ for all Coriolis modes $\boldsymbol{v}_\alpha$ with $\deg\alpha > N$.

## 5. The Coriolis operator with tilted rotation

The rotation is tilted if $0 < \Theta < \pi$. Analytic forms of the tilted geostrophic modes are found in § 5.1, the angular momenta of all Coriolis modes are determined in § 5.2 and conditions for the time independence of the Coriolis operator $\mathcal{C}$ are examined in § 5.3.

### 5.1. *Geostrophic pressure modes in spheroids with tilted rotation*

In terms of $\boldsymbol{D} = (\boldsymbol{ii} + \boldsymbol{jj})/a^2 + \boldsymbol{kk}/c^2$, the surface $\partial V$ and the normal $\boldsymbol{n}$ are $\boldsymbol{r}\cdot\boldsymbol{D}\cdot\boldsymbol{r} = 1$ and $\boldsymbol{n} = \boldsymbol{D}\cdot\boldsymbol{r}$. The rotation, $\widehat{\boldsymbol{\Omega}} = \alpha\boldsymbol{i} + \beta\boldsymbol{j} + \gamma\boldsymbol{k}$ where $\alpha$, $\beta$, $\gamma$ are direction cosines, is tangent to $\partial V$, i.e. $\widehat{\boldsymbol{\Omega}}\cdot\boldsymbol{n} = 0$, at the points of the plane curve, $E_0 := \{\boldsymbol{r} \in E^3 \,|\, \boldsymbol{r}\cdot\boldsymbol{D}\cdot\boldsymbol{r} = 1, \widehat{\boldsymbol{\Omega}}\cdot\boldsymbol{D}\cdot\boldsymbol{r} = 0\}$. The curve $E_0$ is an ellipse lying in the plane $P_0 := \{\boldsymbol{r} \in E^3 \,|\, \widehat{\boldsymbol{\Omega}}\cdot\boldsymbol{D}\cdot\boldsymbol{r} = 0\}$ through the origin with (non-unit) normal $\boldsymbol{N} := \widehat{\boldsymbol{\Omega}}\cdot\boldsymbol{D} = \boldsymbol{D}\cdot\widehat{\boldsymbol{\Omega}} = (\alpha\boldsymbol{i} + \beta\boldsymbol{j})/a^2 + \gamma\boldsymbol{k}/c^2$. Let $H^{-2} := \boldsymbol{N}\cdot\widehat{\boldsymbol{\Omega}} = \widehat{\boldsymbol{\Omega}}\cdot\boldsymbol{D}\cdot\widehat{\boldsymbol{\Omega}} = (\alpha^2 + \beta^2)/a^2 + \gamma^2/c^2$. If $\boldsymbol{N} = |\boldsymbol{N}|(\alpha'\boldsymbol{i} + \beta'\boldsymbol{j} + \gamma'\boldsymbol{k})$, where $|\boldsymbol{N}| = \sqrt{(\alpha^2 + \beta^2)/a^4 + \gamma^2/c^4}$, then $\gamma' = \gamma/c^2|\boldsymbol{N}|$. Thus $\operatorname{sgn}\gamma' = \operatorname{sgn}\gamma$ and $|\gamma'| > |\gamma|$ if $a > c$ or $|\gamma'| < |\gamma|$ if $a < c$. Hence the acute angle between the symmetry axis and $\boldsymbol{N}$ is smaller (greater) than the angle between the symmetry and rotation axes in the oblate (prolate) cases; see figures 5 and 6 respectively.

In the Cartesian coordinates $(x, y, z)$ with the $z$-axis aligned with the symmetry axis of $\partial V$, a point $(x_0, y_0, z_0)$ on $E_0$ is given by the pair of equations

$$\frac{x_0^2 + y_0^2}{a^2} + \frac{z_0^2}{c^2} = 1, \quad \frac{\alpha x_0 + \beta y_0}{a^2} + \frac{\gamma z_0}{c^2} = 0. \tag{5.1a,b}$$

If $\Theta \neq \pi/2$ ($\gamma \neq 0$), eliminating $z_0 = -c^2(\alpha x_0 + \beta y_0)/a^2\gamma$ in (5.1) gives the equation for the perpendicular projection $E_{xy}$ of $E_0$ onto the $xy$-plane,

$$\left(1 + \frac{c^2}{\gamma^2}\frac{\alpha^2}{a^2}\right)\frac{x_0^2}{a^2} + 2\frac{c^2}{\gamma^2}\frac{\alpha x_0}{a^2}\frac{\beta y_0}{a^2} + \left(1 + \frac{c^2}{\gamma^2}\frac{\beta^2}{a^2}\right)\frac{y_0^2}{a^2} = 1, \quad \gamma \neq 0. \tag{5.2}$$

https://doi.org/10.1017/jfm.2017.669 Published online by Cambridge University Press

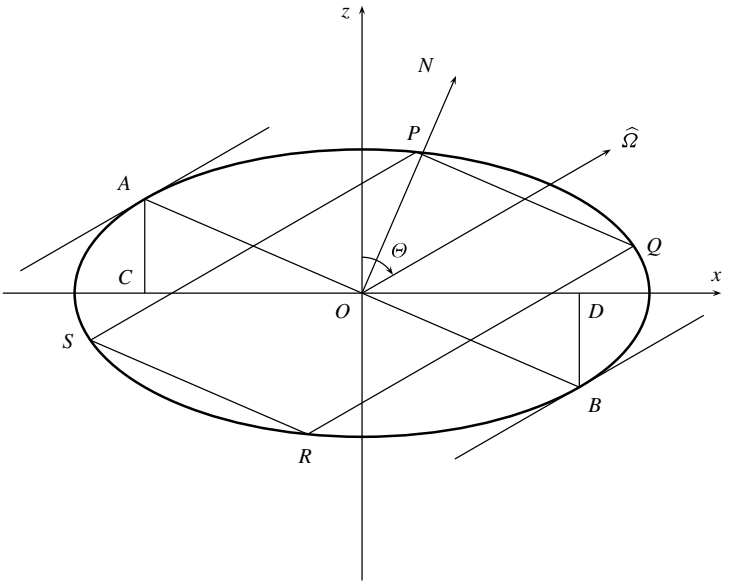



FIGURE 5. Geostrophic cylinder *SPQR* in an oblate spheroid with tilted rotation. The points *C*, *D* are the respective projections of the tangent points *A*, *B* onto the *x*-axis.

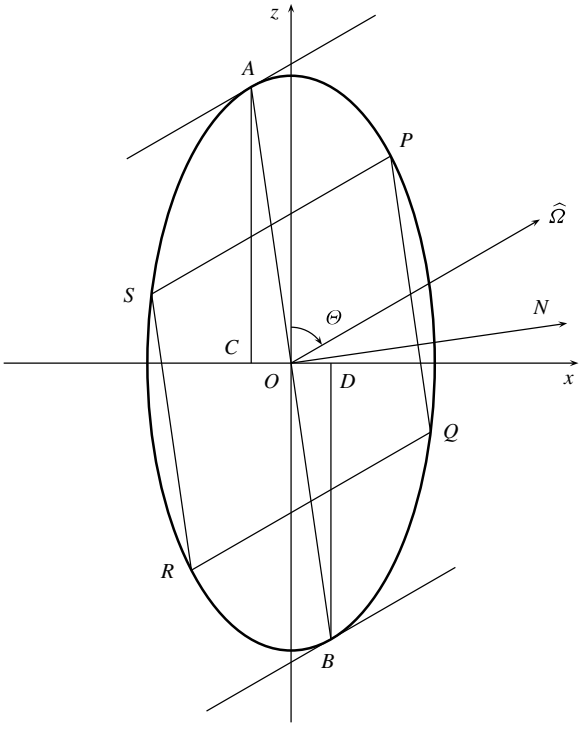



FIGURE 6. Geostrophic cylinder *SPQR* in a prolate spheroid with tilted rotation.

https://doi.org/10.1017/jfm.2017.669 Published online by Cambridge University Press

Thus $E_{xy}$ is also an ellipse. If $\alpha$ or $\beta$ is zero the ellipse $E_{xy}$ is aligned with the $x$- and $y$-axes. If $\Theta \neq 0,\ \pi$ ($\alpha \neq 0$) and allowing $\Theta = \pi/2$ ($\gamma = 0$), eliminating $x_0 = -(\beta y_0 + \gamma z_0 a^2/c^2)/\alpha$ in (5.1) gives the equation for the perpendicular projection $E_{yz}$ of $E_0$ onto an ellipse $E_{yz}$ in the $yz$-plane,

$$\left(1+\frac{\beta^2}{\alpha^2}\right)\frac{y_0^2}{a^2}+2\frac{a^2}{\alpha^2}\frac{\beta y_0}{a^2}\frac{\gamma z_0}{c^2}+\left(1+\frac{a^2}{\alpha^2}\frac{\gamma^2}{c^2}\right)\frac{z_0^2}{c^2}=1,\quad \alpha\neq 0. \tag{5.3}$$

If $\beta$ is zero the ellipse $E_{yz}$ is aligned with the $y$- and $z$-axes.

More generally the oblique projection along $\widehat{\boldsymbol{\Omega}}$ of a point $\boldsymbol{r}$ onto a point $\boldsymbol{r}_0$ in the plane $P_0$ is $\boldsymbol{r} = h\widehat{\boldsymbol{\Omega}} + \boldsymbol{r}_0$, for some $h$. The point $\boldsymbol{r}_0$ lies on or inside the spheroidal surface $\partial V$ if and only if $\boldsymbol{r}_0 \cdot \boldsymbol{D} \cdot \boldsymbol{r}_0 \leqslant 1$. For a given $h$ the associated points $\boldsymbol{r}$ lie in the plane

$$\boldsymbol{N}\cdot\boldsymbol{r} = h\boldsymbol{N}\cdot\widehat{\boldsymbol{\Omega}} + \boldsymbol{N}\cdot\boldsymbol{r}_0 = h\boldsymbol{N}\cdot\widehat{\boldsymbol{\Omega}}. \tag{5.4}$$

and the points $\boldsymbol{r}$ form a curve $\Gamma(h)$ lying on the surface $\partial V$ if and only if

$$1 = \boldsymbol{r}\cdot\boldsymbol{D}\cdot\boldsymbol{r} = h^2\boldsymbol{N}\cdot\widehat{\boldsymbol{\Omega}} + 2h\boldsymbol{N}\cdot\boldsymbol{r}_0 + \boldsymbol{r}_0\cdot\boldsymbol{D}\cdot\boldsymbol{r}_0 = h^2\boldsymbol{N}\cdot\widehat{\boldsymbol{\Omega}} + \boldsymbol{r}_0\cdot\boldsymbol{D}\cdot\boldsymbol{r}_0 \tag{5.5}$$

i.e. $\boldsymbol{r}_0$ satisfies $\boldsymbol{r}_0\cdot\boldsymbol{D}\cdot\boldsymbol{r}_0 = 1 - h^2\boldsymbol{N}\cdot\widehat{\boldsymbol{\Omega}}$. Thus the geostrophic contours are given by

$$\Gamma(h) := \{\boldsymbol{r}\in E^3 \mid \boldsymbol{r} = h\widehat{\boldsymbol{\Omega}} + \boldsymbol{r}_0;\ \boldsymbol{r}_0\cdot\boldsymbol{D}\cdot\boldsymbol{r}_0 = 1 - h^2\boldsymbol{N}\cdot\widehat{\boldsymbol{\Omega}},\ \boldsymbol{N}\cdot\boldsymbol{r}_0 = 0\}, \tag{5.6}$$

where $|h| \leqslant H = (\boldsymbol{N}\cdot\widehat{\boldsymbol{\Omega}})^{-1/2}$. There is a geostrophic contour through every point on $\partial V$: given $\boldsymbol{r}\in\partial V$, then $h = \boldsymbol{N}\cdot\boldsymbol{r}/\boldsymbol{N}\cdot\widehat{\boldsymbol{\Omega}}$ and $\boldsymbol{r}_0 = \boldsymbol{r} - h\widehat{\boldsymbol{\Omega}}$ satisfies the conditions in the definition (5.6). The contours $\Gamma(\pm h)$ are parallel and form the ends of a geostrophic cylinder of height $2|h|$, which intersects the plane $P_0$ in the ellipse $E_{|h|} := \{\boldsymbol{r}_0\in E^3 \mid \boldsymbol{r}_0\cdot\boldsymbol{D}\cdot\boldsymbol{r}_0 = 1 - h^2\boldsymbol{N}\cdot\widehat{\boldsymbol{\Omega}},\ \boldsymbol{N}\cdot\boldsymbol{r}_0 = 0\}$. There is a unique ellipse $E_{|h|}$ through any point $\boldsymbol{r}_0\in P_0$ which lies inside $E_0$, in fact, $|h| = [(1 - \boldsymbol{r}\cdot\boldsymbol{D}\cdot\boldsymbol{r})/\boldsymbol{N}\cdot\widehat{\boldsymbol{\Omega}}]^{1/2}$.

If $\Theta \neq \pi/2$ the perpendicular projection of the ellipse $E_{|h|}$ onto the $xy$-plane is the ellipse $E_{xy}(|h|)$ given by the equation

$$\left(1+\frac{c^2}{\gamma^2}\frac{\alpha^2}{a^2}\right)\frac{x_0^2}{a^2}+2\frac{c^2}{\gamma^2}\frac{\alpha x_0}{a^2}\frac{\beta y_0}{a^2}+\left(1+\frac{c^2}{\gamma^2}\frac{\beta^2}{a^2}\right)\frac{y_0^2}{a^2}=1-\frac{h^2}{H^2},\quad \gamma\neq 0. \tag{5.7}$$

If $\Theta \neq 0, \pi$ ($\alpha \neq 0$) the projection of $E_{|h|}$ onto the $yz$-plane is the ellipse $E_{yz}(|h|)$ given by

$$\left(1+\frac{\beta^2}{\alpha^2}\right)\frac{y_0^2}{a^2}+2\frac{a^2}{\alpha^2}\frac{\beta y_0}{a^2}\frac{\gamma z_0}{c^2}+\left(1+\frac{a^2}{\alpha^2}\frac{\gamma^2}{c^2}\right)\frac{z_0^2}{c^2}=1-\frac{h^2}{H^2},\quad \alpha\neq 0. \tag{5.8}$$

In figures 5 and 6 the projections onto the $xz$-plane of $E_0$, $E_{xy}$, geostrophic contours and a geostrophic cylinder are given by $AB$, $CD$, $PQ$, $RS$ and $PQRS$ respectively.

For a spheroid $b = a$ and the $x$-axis can be chosen so that $\widehat{\boldsymbol{\Omega}}$ lies in the first quadrant of the $xz$-plane, i.e. $\boldsymbol{j}\cdot\widehat{\boldsymbol{\Omega}} = \beta = 0$ and $\alpha \geqslant 0$. Also $\boldsymbol{j}\cdot\widehat{\boldsymbol{N}} = \beta/a^2 = 0$. As above, let $\boldsymbol{r}$ be a point in $E^3$. In terms of the basis $(\boldsymbol{j}\times\widehat{\boldsymbol{N}}, \boldsymbol{j}, \widehat{\boldsymbol{\Omega}})$, $\boldsymbol{r} = X\boldsymbol{j}\times\widehat{\boldsymbol{N}} + Y\boldsymbol{j} + Z\widehat{\boldsymbol{\Omega}}$. The vectors reciprocal to $(\boldsymbol{j}\times\widehat{\boldsymbol{N}}, \boldsymbol{j}, \widehat{\boldsymbol{\Omega}})$ are $(J^{-1}\boldsymbol{j}\times\widehat{\boldsymbol{\Omega}}, \boldsymbol{j}, J^{-1}\widehat{\boldsymbol{N}})$, where the Jacobian $J = (\boldsymbol{j}\times\widehat{\boldsymbol{N}})\times\boldsymbol{j}\cdot$

https://doi.org/10.1017/jfm.2017.669 Published online by Cambridge University Press

$\widehat{\boldsymbol{\Omega}} = \widehat{\boldsymbol{\Omega}} \cdot \widehat{\boldsymbol{N}} = (H^2|\boldsymbol{N}|)^{-1}$ and now $H^{-1} = \sqrt{\alpha^2/a^2 + \gamma^2/c^2}$ and $|\boldsymbol{N}| = \sqrt{\alpha^2/a^4 + \gamma^2/c^4}$. Thus $X = J^{-1}\boldsymbol{j} \times \widehat{\boldsymbol{\Omega}} \cdot \boldsymbol{r}$, $Y = \boldsymbol{j} \cdot \boldsymbol{r}$, $Z = J^{-1}\widehat{\boldsymbol{N}} \cdot \boldsymbol{r}$, i.e.

$$X = H^2|\boldsymbol{N}|(\gamma x - \alpha z), \quad Y = y, \quad Z = H^2(\alpha x/a^2 + \gamma z/c^2). \tag{5.9a–c}$$

In particular, the oblique projection $(x_0, y_0, z_0)$ of $(x, y, z)$ onto the plane $P_0$ is the point given by $X = |\boldsymbol{N}|c^2 x_0/\gamma = -|\boldsymbol{N}|a^2 z_0/\alpha$, $Y = y_0$, $Z = 0$. Thus, solving (5.7) if $\gamma \neq 0$, or (5.8) if $\alpha \neq 0$, for $h$ gives

$$h = H\left(1 - \frac{X^2}{H^2|\boldsymbol{N}|^2 a^2 c^2} - \frac{Y^2}{a^2}\right)^{1/2}. \tag{5.10}$$

The geostrophic flow due to the pressure $P$ is $\boldsymbol{v} = [\widehat{\boldsymbol{\Omega}} - \boldsymbol{\nabla}(1/2)(z_t + z_b)] \times \boldsymbol{\nabla} P = P'(h)\boldsymbol{t}$, where $z_t$ and $z_b$ are the values of $z$ on $\Gamma(\pm h)$, $P$ depends only the height $h$ of the geostrophic cylinders and $\boldsymbol{t} := \boldsymbol{\nabla} Z \times \boldsymbol{\nabla} h$ is tangent to the streamlines of $\boldsymbol{v}$ noting $Z = z - (1/2)(z_t + z_b)$ (see Ivers *et al.* 2015, equation (3.9)). The gradient in the non-orthogonal coordinates $(X, Y, Z)$ is $\boldsymbol{\nabla} = J^{-1}\boldsymbol{j} \times \widehat{\boldsymbol{\Omega}}\,\partial_X + \boldsymbol{j}\,\partial_Y + J^{-1}\widehat{\boldsymbol{N}}\,\partial_Z$; in particular $\boldsymbol{\nabla} Z = J^{-1}\widehat{\boldsymbol{N}}$. Since $h$ is independent of $Z$, $\boldsymbol{\nabla} h = J^{-1}\boldsymbol{j} \times \widehat{\boldsymbol{\Omega}}\,\partial_X h + \boldsymbol{j}\,\partial_Y h$ and

$$\boldsymbol{\nabla} h = -H^2\left(\boldsymbol{j} \times \widehat{\boldsymbol{\Omega}}\,\frac{X}{|\boldsymbol{N}|a^2c^2h} + \boldsymbol{j}\,\frac{Y}{a^2 h}\right). \tag{5.11}$$

Thus the geostrophic flow due to the pressure $P(h)$ is

$$\boldsymbol{v} = \frac{H^2 P'(h)}{a^2 h}\left(\boldsymbol{j} \times \boldsymbol{N} H^2 Y - \boldsymbol{j}\,\frac{X}{|\boldsymbol{N}|c^2}\right). \tag{5.12}$$

If $P(h)$ is a polynomial in $x, y, z$ and hence a polynomial in $X, Y, Z$, then it must be a polynomial in $h$ of even degree and hence of even degree in $x, y, z$. The ratio $P'(h)/h$ is a polynomial in $h$ of even degree and if $\deg P(h) = n$ then the velocity in (5.10) is a polynomial in $x, y, z$ of odd degree $n - 1$. For $n = 2$ the linear geostrophic mode $\boldsymbol{v}_{1,0}$ in (3.29) is recovered up to normalisation and phase. To complete the derivation of the geostrophic modes a natural polynomial basis for the geostrophic pressure modes can be constructed using the inner product of two geostrophic velocity modes $\boldsymbol{v}_1$ and $\boldsymbol{v}_2$ with pressures $P_1$ and $P_2$,

$$(\boldsymbol{v}_1, \boldsymbol{v}_2) = \int_V \frac{\mathrm{d}P_1}{\mathrm{d}h}\frac{\mathrm{d}P_2^*}{\mathrm{d}h}\,\boldsymbol{t}^2\,\mathrm{d}V. \tag{5.13}$$

Let $X = aAs\cos\phi$ and $Y = as\sin\phi$, where $A := H|\boldsymbol{N}|c$, then $h = H\sqrt{1 - s^2}$ and

$$\boldsymbol{t}^2 = \frac{H^4}{a^2 h^2}\left(\frac{H^2}{c^2}\cos^2\phi + |\boldsymbol{N}|^2 H^4 \sin^2\phi\right)s^2. \tag{5.14}$$

Also $\mathrm{d}X\,\mathrm{d}Y = a^2 As\,\mathrm{d}s\,\mathrm{d}\phi$ so that $\mathrm{d}V = J\,\mathrm{d}X\,\mathrm{d}Y\,\mathrm{d}Z = a^2 cs\,\mathrm{d}s\,\mathrm{d}\phi\,\mathrm{d}Z$. Assuming $P_1$ and $P_2$ are real (5.13) implies

$$(\boldsymbol{v}_1, \boldsymbol{v}_2) = 2cH^4\int_0^1 \frac{\mathrm{d}P_1}{\mathrm{d}h}\frac{\mathrm{d}P_2}{\mathrm{d}h}\frac{s^3\,\mathrm{d}s}{h}\oint\left(\frac{H^2}{c^2}\cos^2\phi + |\boldsymbol{N}|^2 H^4\sin^2\phi\right)\mathrm{d}\phi. \tag{5.15}$$

https://doi.org/10.1017/jfm.2017.669 Published online by Cambridge University Press

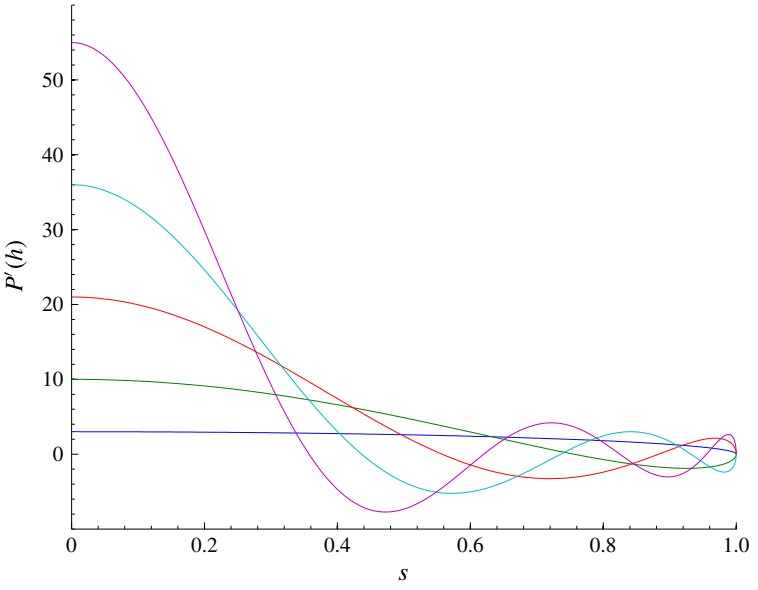



FIGURE 7. (Colour online) Geostrophic velocity modes of degrees 1, 3, 5, 7, 9.

Let $v^2 = 1 - s^2$, then $v = h/H$ and $P_1$, $P_2$ are polynomials of even degree in $v$. Thus

$$(\boldsymbol{v}_1, \boldsymbol{v}_2) = \pi cH(|\boldsymbol{N}|^2H^4 + H^2/c^2) \int_{-1}^{1} \frac{\mathrm{d}P_1}{\mathrm{d}v}\frac{\mathrm{d}P_2}{\mathrm{d}v}(1 - v^2)\,\mathrm{d}v. \tag{5.16}$$

The orthogonal polynomial pressure modes are thus $P_{n,0}(h) = P_n(h/H)$, i.e. using (5.9) and (5.10)

$$P_{n,0}(x, y, z) = P_n([1 - (\gamma x - \alpha z)^2(H/ac)^2 - y^2/a^2]^{1/2}), \tag{5.17}$$

where $n$ is a positive even integer and $P_n$ is a Legendre polynomial of degree $n$. Thus from (5.12) the tilted geostrophic velocity modes have a universal radial structure in terms of $s$ given by $P_n'(\sqrt{1 - s^2})$. The $n/2$th mode consists of a central rotating core surrounded by $(1/2)n - 1$ flows of alternating directions. The first five modes are shown in figure 7. As $\alpha \to 0$ and $\gamma \to 1$, $h/H \to \sqrt{1 - (x^2 + y^2)/a^2}$, since $H \to c$; this agrees with the aligned geostrophic modes (2.18) and linear mode (3.29) up to an additive constant and normalisation.

### 5.2. *The angular momenta of spheroidal Coriolis modes*

Let $\boldsymbol{L}_\alpha \mathrm{e}^{-\mathrm{i}\omega_\alpha t}$ denote the angular momentum of the Coriolis mode $\boldsymbol{v}_\alpha$ in the boundary frame, where the spatially dependent part $\boldsymbol{L}_\alpha := \int_V \boldsymbol{r} \times \boldsymbol{v}_\alpha \,\mathrm{d}V$.

THEOREM 5.1. *If $\boldsymbol{v}_\alpha$ is a Coriolis mode of degree greater than one, the angular momentum of $\boldsymbol{v}_\alpha$ in the boundary frame vanishes, i.e. $\boldsymbol{L}_\alpha = \boldsymbol{0}$ if $\deg \alpha > 1$. The angular momenta of the degree-one modes, $\boldsymbol{v}_{1,0}$ and $\boldsymbol{v}_{1,\pm\omega_1}$, in the boundary frame are*

$$\boldsymbol{L}_{1,0} = \frac{\alpha c^2/a^2\boldsymbol{i} + \gamma\boldsymbol{k}}{(1 + c^2/a^2)^2\omega_1^2 T_{1,0}}, \qquad \boldsymbol{L}_{1,\pm\omega_1} = \frac{[-\gamma/(1 + c^2/a^2)\boldsymbol{i} \pm \mathrm{i}\omega_1\boldsymbol{j} + \frac{1}{2}\alpha\boldsymbol{k}]c/a}{(1 + c^2/a^2)\omega_1^2 T_{1,\omega_1}}. \tag{5.18a,b}$$

https://doi.org/10.1017/jfm.2017.669 Published online by Cambridge University Press

*Proof.* The representation $\boldsymbol{c}\times\boldsymbol{r}=\boldsymbol{v}_c-\boldsymbol{\nabla}\pi$, where $\boldsymbol{c}$ is a constant vector and $\boldsymbol{v}_c\in\mathcal{P}_1(V)$, is explicitly constructed below as follows, from $\nabla^2\pi=-\boldsymbol{\nabla}\cdot(\boldsymbol{c}\times\boldsymbol{r})=0$ in $V$ and $\boldsymbol{n}\cdot\boldsymbol{\nabla}\pi=-\boldsymbol{n}\cdot\boldsymbol{c}\times\boldsymbol{r}$ on $\partial V$. To solve these equations assume that the pressure $\pi=(1/2)\boldsymbol{r}\cdot\boldsymbol{P}\cdot\boldsymbol{r}+\boldsymbol{q}\cdot\boldsymbol{r}$, where $\boldsymbol{P}$ is a constant symmetric matrix and $\boldsymbol{q}$ is a constant vector (new from § 3.2). Thus $\boldsymbol{\nabla}\pi=\boldsymbol{P}\cdot\boldsymbol{r}+\boldsymbol{q}$ and $\nabla^2\pi=\operatorname{tr}\boldsymbol{P}=0$. Since the normal $\boldsymbol{n}=\boldsymbol{D}\cdot\boldsymbol{r}$,

$$\boldsymbol{r}\cdot\boldsymbol{D}\cdot(\boldsymbol{P}+\boldsymbol{c}\times\boldsymbol{I})\cdot\boldsymbol{r}+\boldsymbol{r}\cdot\boldsymbol{D}\cdot\boldsymbol{q}=0 \tag{5.19}$$

on the boundary $\partial V$ where $\boldsymbol{r}\cdot\boldsymbol{D}\cdot\boldsymbol{r}=1$. Replacing $\boldsymbol{r}$ by $-\boldsymbol{r}$ in (5.19) implies $\boldsymbol{q}=\boldsymbol{0}$, which leaves $\boldsymbol{r}\cdot\boldsymbol{D}\cdot(\boldsymbol{P}+\boldsymbol{c}\times\boldsymbol{I})\cdot\boldsymbol{r}=0$ subject to $\boldsymbol{r}\cdot\boldsymbol{D}\cdot\boldsymbol{r}=1$. Scaling $\boldsymbol{r}$ the inhomogeneous condition can be replaced by $\boldsymbol{r}\cdot\boldsymbol{D}\cdot\boldsymbol{r}\neq0$, i.e. by $\boldsymbol{r}\neq\boldsymbol{0}$ since $\boldsymbol{D}$ is positive definite, and hence discarded completely. Thus the symmetric part of $\boldsymbol{D}\cdot(\boldsymbol{P}+\boldsymbol{c}\times\boldsymbol{I})$ must vanish. In Cartesian matrix form

$$\boldsymbol{D}\cdot(\boldsymbol{P}+\boldsymbol{c}\times\boldsymbol{I})=\begin{pmatrix}P_{11}/a^2 & (P_{12}-c_3)/a^2 & (P_{13}+c_2)/a^2\\ (P_{21}+c_3)/a^2 & P_{22}/a^2 & (P_{23}-c_1)/a^2\\ (P_{31}-c_2)/c^2 & (P_{32}+c_1)/c^2 & P_{33}/c^2\end{pmatrix}. \tag{5.20}$$

Since the symmetric part of the matrix vanishes, $P_{11}=P_{22}=P_{33}=P_{12}=P_{21}=0$ and

$$P_{13}=P_{31}=\frac{a^2-c^2}{a^2+c^2}c_2,\quad P_{23}=P_{32}=-\frac{a^2-c^2}{a^2+c^2}c_1. \tag{5.21a,b}$$

Hence

$$\pi=\frac{a^2-c^2}{a^2+c^2}(c_2x-c_1y)z \tag{5.22}$$

and $\boldsymbol{v}_c=c_1\boldsymbol{v}_i+c_2\boldsymbol{v}_j+c_3\boldsymbol{v}_k$, where

$$\boldsymbol{v}_i:=-\frac{2(a^2z\boldsymbol{j}-c^2y\boldsymbol{k})}{a^2+c^2},\quad \boldsymbol{v}_j:=\frac{2(a^2z\boldsymbol{i}-c^2x\boldsymbol{k})}{a^2+c^2},\quad \boldsymbol{v}_k:=-y\boldsymbol{i}+x\boldsymbol{j} \tag{5.23a–c}$$

are the flows for $\boldsymbol{c}=\boldsymbol{i},\boldsymbol{j},\boldsymbol{k}$. It is easily checked that $\boldsymbol{\nabla}\cdot\boldsymbol{v}_c=0$ in $V$ and $\boldsymbol{n}\cdot\boldsymbol{v}_c=0$ on $\partial V$. The flow $\boldsymbol{v}_c$ is a linear combination of the linear Coriolis modes (3.29) and (3.30), since

$$\boldsymbol{v}_i=\frac{c/a}{(1+c^2/a^2)^2\omega_1^2}\left(-\frac{\gamma}{T_{1,\omega_1}}\boldsymbol{v}_{1,-\omega_1}+\frac{\alpha c}{aT_{1,0}}\boldsymbol{v}_{1,0}-\frac{\gamma}{T_{1,\omega_1}}\boldsymbol{v}_{1,\omega_1}\right) \tag{5.24}$$

$$\boldsymbol{v}_j=-\mathrm{i}\frac{c/a}{(1+c^2/a^2)\omega_1}\left(-\frac{1}{T_{1,\omega_1}}\boldsymbol{v}_{1,-\omega_1}+\frac{1}{T_{1,\omega_1}}\boldsymbol{v}_{1,\omega_1}\right) \tag{5.25}$$

$$\boldsymbol{v}_k=\frac{1}{2(1+c^2/a^2)\omega_1^2}\left(\frac{\alpha c}{aT_{1,\omega_1}}\boldsymbol{v}_{1,-\omega_1}+\frac{2\gamma}{(1+c^2/a^2)T_{1,0}}\boldsymbol{v}_{1,0}+\frac{\alpha c}{aT_{1,\omega_1}}\boldsymbol{v}_{1,\omega_1}\right). \tag{5.26}$$

Let $\boldsymbol{c}$ be a real unit vector. The component of $\boldsymbol{L}_\alpha$ in the direction $\boldsymbol{c}$ is

$$\boldsymbol{c}\cdot\boldsymbol{L}_\alpha=\int_V\boldsymbol{c}\times\boldsymbol{r}\cdot\boldsymbol{v}_\alpha\,\mathrm{d}V=(\boldsymbol{v}_\alpha,\boldsymbol{c}\times\boldsymbol{r})=(\boldsymbol{v}_\alpha,\boldsymbol{v}_c)-(\boldsymbol{v}_\alpha,\boldsymbol{\nabla}\pi)=(\boldsymbol{v}_\alpha,\boldsymbol{v}_c). \tag{5.27}$$

Since the degree of $\boldsymbol{v}_c$ is one and $\boldsymbol{c}$ is arbitrary, $\boldsymbol{L}_\alpha=\boldsymbol{0}$ if $\deg\alpha>1$.

For the degree-one modes, $\boldsymbol{i}\cdot\boldsymbol{L}_{1,0}=(\boldsymbol{v}_{1,0},\boldsymbol{v}_i)=(\boldsymbol{v}_i,\boldsymbol{v}_{1,0})^*=\alpha c^2/[a^2(1+c^2/a^2)^2\omega_1^2T_{1,0}]$, by (5.24) and (5.27). The $y$ and $z$ components of $\boldsymbol{L}_{1,0}$, and $\boldsymbol{L}_{1,\pm\omega_1}$ are found similarly. Thus equations (5.18) hold. □

https://doi.org/10.1017/jfm.2017.669 Published online by Cambridge University Press

### 5.3. *Dynamics of the rigid spheroidal boundary*

We now examine conditions under which the angular velocity of the boundary frame is constant, i.e. $\dot{\boldsymbol{\Omega}} = \boldsymbol{0}$, and hence $\mathcal{C}$ is time independent. Assume $V$ is surrounded by a rigid mantle $M$ fixed in the boundary frame of $\partial V$ with the centre of mass of $M$ at the centre $O$ of $V$, which is stationary in the inertial frame $O'$ introduced in § 1, and moment of inertia tensor $\boldsymbol{I}_M$. Thus the angular velocity of $M$ is $\boldsymbol{\Omega}$. The angular momenta of $M$ relative to the boundary frame $\boldsymbol{L}_M$ and the inertial frame $\boldsymbol{L}'_M$ are $\boldsymbol{L}_M = \boldsymbol{0}$ and $\boldsymbol{L}'_M = \boldsymbol{I}_M \cdot \boldsymbol{\Omega}$.

If $\dot{\boldsymbol{\Omega}} \neq \boldsymbol{0}$ the dimensional inviscid non-magnetic momentum equation with variable density $\rho$ in the rotating boundary frame is

$$\rho D_t \boldsymbol{v} + \rho 2\boldsymbol{\Omega} \times \boldsymbol{v} + \rho \boldsymbol{\Omega} \times (\boldsymbol{\Omega} \times \boldsymbol{r}) + \rho \dot{\boldsymbol{\Omega}} \times \boldsymbol{r} = -\boldsymbol{\nabla} p - \rho \boldsymbol{\nabla} U. \tag{5.28}$$

Let $\boldsymbol{L}_V$ and $\boldsymbol{I}_V$ be the angular momentum and the inertia tensor of the fluid volume $V$ in the boundary frame: $\boldsymbol{L}_V := \int_V \boldsymbol{r} \times \rho \boldsymbol{v} \, \mathrm{d}V$ and $\boldsymbol{I}_V := \int_V \rho (r^2 \boldsymbol{I} - \boldsymbol{rr}) \, \mathrm{d}V$. The identities $D_t(r^2 \boldsymbol{I} - \boldsymbol{rr}) = 2\boldsymbol{r} \cdot \boldsymbol{v} \boldsymbol{I} - \boldsymbol{rv} - \boldsymbol{vr}$, $\boldsymbol{r} \times (\dot{\boldsymbol{\Omega}} \times \boldsymbol{r}) = (r^2 \boldsymbol{I} - \boldsymbol{rr}) \cdot \dot{\boldsymbol{\Omega}}$ and

$$\frac{\mathrm{d}\boldsymbol{I}_V}{\mathrm{d}t} = \int_V \rho D_t (r^2 \boldsymbol{I} - \boldsymbol{rr}) \, \mathrm{d}V, \tag{5.29}$$

noting $\boldsymbol{v} \cdot \boldsymbol{n} = 0$ on $\partial V$ in the boundary frame, yield the following identity for the moments of the Coriolis force $\rho 2\boldsymbol{\Omega} \times \boldsymbol{v}$ and the Poincaré force $\rho \dot{\boldsymbol{\Omega}} \times \boldsymbol{r}$,

$$\frac{\mathrm{d}(\boldsymbol{\Omega} \cdot \boldsymbol{I}_V)}{\mathrm{d}t} + \boldsymbol{\Omega} \times \boldsymbol{L}_V = \int_V \boldsymbol{r} \times \rho (2\boldsymbol{\Omega} \times \boldsymbol{v} + \dot{\boldsymbol{\Omega}} \times \boldsymbol{r}) \, \mathrm{d}V. \tag{5.30}$$

Also, by Reynolds transport theorem,

$$\frac{\mathrm{d}\boldsymbol{L}_V}{\mathrm{d}t} = \int_V \rho D_t (\boldsymbol{r} \times \boldsymbol{v}) \, \mathrm{d}V = \int_V \boldsymbol{r} \times \rho D_t \boldsymbol{v} \, \mathrm{d}V. \tag{5.31}$$

Substituting the momentum equation (5.28) yields

$$\frac{\mathrm{d}\boldsymbol{L}_V}{\mathrm{d}t} + \boldsymbol{I}_V \cdot \dot{\boldsymbol{\Omega}} + \boldsymbol{\Omega} \times (\boldsymbol{I}_V \cdot \boldsymbol{\Omega}) = -\int_V \boldsymbol{r} \times \rho (2\boldsymbol{\Omega} \times \boldsymbol{v} + \rho^{-1} \boldsymbol{\nabla} p + \boldsymbol{\nabla} U) \, \mathrm{d}V. \tag{5.32}$$

Adding (5.29) and (5.30) eliminates the Coriolis torque and yields

$$\frac{\mathrm{d}\boldsymbol{L}'_V}{\mathrm{d}t'} = -\int_{\partial V} \boldsymbol{r} \times p \, \mathrm{d}\boldsymbol{S} - \int_V \boldsymbol{r} \times \rho \boldsymbol{\nabla} U \, \mathrm{d}V, \tag{5.33}$$

in the inertial frame $O'$, where $\boldsymbol{L}'_V = \boldsymbol{I}_V \cdot \boldsymbol{\Omega} + \boldsymbol{L}_V$ and $\mathrm{d}/\mathrm{d}t' \equiv \mathrm{d}/\mathrm{d}t + \boldsymbol{\Omega} \times$ is the vector time derivative in the inertial frame.

If $\rho$ is uniform in $V$, then from (5.29)

$$\frac{\mathrm{d}\boldsymbol{I}_V}{\mathrm{d}t} = \rho \int_V \boldsymbol{v} \cdot \boldsymbol{\nabla} (r^2 \boldsymbol{I} - \boldsymbol{rr}) \, \mathrm{d}V = \rho \int_{\partial V} \mathrm{d}\boldsymbol{S} \cdot \boldsymbol{v} (r^2 \boldsymbol{I} - \boldsymbol{rr}) = \boldsymbol{0}, \tag{5.34}$$

i.e. the inertia tensor $\boldsymbol{I}_V$ is constant in the boundary frame if the fluid density is uniform. Of course, then $\mathrm{d}\boldsymbol{I}_V/\mathrm{d}t' = \boldsymbol{\Omega} \times \boldsymbol{I}_V - \boldsymbol{I}_V \times \boldsymbol{\Omega} \neq \boldsymbol{0}$. Also, by (5.33),

$$\frac{\mathrm{d}\boldsymbol{L}'_V}{\mathrm{d}t'} = -\int_{\partial V} \boldsymbol{r} \times P \, \mathrm{d}\boldsymbol{S}, \tag{5.35}$$

https://doi.org/10.1017/jfm.2017.669 Published online by Cambridge University Press

where $P = p + \rho U$, since $\boldsymbol{r} \times \rho \nabla U = \nabla \times \rho U \boldsymbol{r}$. In general, $P$ is not the pressure auxiliary to $\mathcal{C}\boldsymbol{v}$. For the rigid mantle $M$,

$$\frac{\mathrm{d}\boldsymbol{L}'_M}{\mathrm{d}t'} = \int_{\partial V} \boldsymbol{r} \times P \,\mathrm{d}\boldsymbol{S} + \boldsymbol{\Gamma}_M, \tag{5.36}$$

where $\boldsymbol{\Gamma}_M$ is the torque on $M$ external to $M \cup V$, by Newton's laws. There is no requirement for $M$ to be a homeoidal shell or for Ivory's theorem as the mutual gravitational torque is contained in the surface pressure torque over $\partial V$. Adding (5.35) and (5.36) gives $\mathrm{d}(\boldsymbol{L}'_V + \boldsymbol{L}'_M)/\mathrm{d}t' = \boldsymbol{\Gamma}_M$ or, since $M$ is rigid,

$$(\boldsymbol{I}_V + \boldsymbol{I}_M) \cdot \dot{\boldsymbol{\Omega}} = \boldsymbol{\Gamma}_M - \boldsymbol{\Omega} \times (\boldsymbol{I}_V + \boldsymbol{I}_M) \cdot \boldsymbol{\Omega} - \frac{\mathrm{d}\boldsymbol{L}_V}{\mathrm{d}t} - \boldsymbol{\Omega} \times \boldsymbol{L}_V. \tag{5.37}$$

Thus $\dot{\boldsymbol{\Omega}} = \boldsymbol{0}$ if $\boldsymbol{\Gamma}_M$ balances the terms on the right-hand side,

$$\boldsymbol{\Gamma}_M = \boldsymbol{\Omega} \times (\boldsymbol{I}_V + \boldsymbol{I}_M) \cdot \boldsymbol{\Omega} + \frac{\mathrm{d}\boldsymbol{L}_V}{\mathrm{d}t} + \boldsymbol{\Omega} \times \boldsymbol{L}_V. \tag{5.38}$$

In a laboratory $\boldsymbol{\Gamma}_M$ must be supplied by the bearings supporting $V \cup M$. Given $\boldsymbol{I}_V$ the boundary inertia tensor $\boldsymbol{I}_M$ can be adjusted such that $\boldsymbol{I}_V + \boldsymbol{I}_M$ is diagonal, i.e. $\boldsymbol{I}_V + \boldsymbol{I}_M = A\boldsymbol{ii} + B\boldsymbol{jj} + C\boldsymbol{kk}$, even isotropic with $A = B = C$, to minimise $\boldsymbol{\Gamma}_M$. The inertia tensor of the spheroid about its centre is $\boldsymbol{I}_V = (1/5)M[(a^2 + c^2)(\boldsymbol{ii} + \boldsymbol{jj}) + 2a^2\boldsymbol{kk}]$. If $V$ is oblate ($c < a$) the inertia tensor of a dumbbell $D := \{(0, 0, -c), (0, 0, c)\}$ of mass $(1/10)M(a^2 - c^2)/c^2$ is $\boldsymbol{I}_D = (1/10)M(a^2 - c^2)\boldsymbol{kk}$. Then, neglecting the inertial of the surface material, $\boldsymbol{I}_V + \boldsymbol{I}_M = \boldsymbol{I}_V + \boldsymbol{I}_D = (2/5)Ma^2\boldsymbol{I}$. Similarly, if $V$ is prolate ($c > a$), then the inertia tensor of a uniform ring $R := \{(x, y, z) \mid x^2 + y^2 = a^2, z = 0\}$ of mass $(2/5)M(c^2 - a^2)/a^2$ is $\boldsymbol{I}_R = (1/5)M(c^2 - a^2)(\boldsymbol{ii} + \boldsymbol{jj} + 2\boldsymbol{kk})$ and $\boldsymbol{I}_V + \boldsymbol{I}_R = (2/5)Mc^2\boldsymbol{I}$. The external torque necessary for $\dot{\boldsymbol{\Omega}} = \boldsymbol{0}$ reduces to $\boldsymbol{\Gamma}_M = \mathrm{d}\boldsymbol{L}_V/\mathrm{d}t + \boldsymbol{\Omega} \times \boldsymbol{L}_V$, which is zero for any superposition of Coriolis modes excluding the degree one modes. If the superposition includes degree-one modes, then $\mathrm{d}\boldsymbol{L}_V/\mathrm{d}t + \boldsymbol{\Omega} \times \boldsymbol{L}_V$ and hence $\boldsymbol{\Gamma}_M$ are non-zero.

For large objects such as the Earth the external torque $\boldsymbol{\Gamma}_M$ is not a control and $\boldsymbol{I}_M$ is not adjustable. Note the term $\boldsymbol{\Omega} \times (\boldsymbol{I}_V + \boldsymbol{I}_M) \cdot \boldsymbol{\Omega}$ vanishes if $(\boldsymbol{I}_V + \boldsymbol{I}_M) \cdot \boldsymbol{\Omega} = \lambda\boldsymbol{\Omega}$ for some scalar $\lambda$, i.e. $\boldsymbol{\Omega}$ is an eigenvector of $\boldsymbol{I}_V + \boldsymbol{I}_M$. This implies that $\boldsymbol{I}_V + \boldsymbol{I}_M$ must be isotropic, if $\boldsymbol{\Omega}$ is tilted from the principal axes of $\partial V$, or if $\boldsymbol{I}_V + \boldsymbol{I}_M$ is anisotropic, that $\boldsymbol{\Omega}$ must be aligned with a principal axis of $\partial V$. It may be that $\dot{\boldsymbol{\Omega}}$ is small so that the dominant part of $\boldsymbol{\Omega}$ is constant. If $A$, $B$, $C$ are now the principal moments of inertia of $\boldsymbol{I}_V + \boldsymbol{I}_M$, $\dot{\boldsymbol{\Omega}}$ can be estimated from (5.37): thus $|\dot{\boldsymbol{\Omega}}|/|\boldsymbol{\Omega}|^2 \ll 1$ if $|\boldsymbol{\Gamma}_M| \ll \min(A, B, C)|\boldsymbol{\Omega}|^2$, $\max(|B - C|/A, |A - C|/B, |A - B|/C) \ll 1$, $|\boldsymbol{L}_V| \ll \min(A, B, C)|\boldsymbol{\Omega}|$. For the Earth $\dot{\boldsymbol{\Omega}} \approx \boldsymbol{\Omega}_p \times \boldsymbol{\Omega}$, where the rate of precession $|\boldsymbol{\Omega}_p| = 7.7260 \times 10^{-12}$ rad s$^{-1}$ and $|\boldsymbol{\Omega}| = 7.292115 \times 10^{-5}$ rad s$^{-1}$ (Stacey & Davis 2008). Thus $|\dot{\boldsymbol{\Omega}}|/|\boldsymbol{\Omega}|^2 \sim |\boldsymbol{\Omega}_p|/|\boldsymbol{\Omega}| \approx 10^{-7}$.

### 5.4. *Stokes and other operators in Coriolis bases*

A second useful operator associated with the Navier–Stokes equation (1.2) is the Stokes operator,

$$\mathcal{S}\boldsymbol{v} := -\nabla^2\boldsymbol{v} + \nabla p \tag{5.39}$$

with $\nabla^2 p = 0$ in $V$, $\boldsymbol{n} \cdot \nabla p = \boldsymbol{n} \cdot \nabla^2\boldsymbol{v}$ on $\partial V$. By Theorem 4.2 $\mathcal{S}$ maps a flow $\boldsymbol{v} \in \mathcal{P}^n(V)$ into $\mathcal{P}^{n-2}(V)$ and thus $(\mathcal{S}\boldsymbol{v}, \boldsymbol{v}_\alpha) = 0$ for any $\boldsymbol{v}_\alpha$ with $\deg \alpha \geqslant n - 1$, and

https://doi.org/10.1017/jfm.2017.669 Published online by Cambridge University Press

hence $(\nabla^2 \boldsymbol{v}_\beta, \boldsymbol{v}_\alpha) = 0$ if $\deg\beta \leqslant \deg\alpha + 1$. This extends the spheroidal result of Zhang *et al.* (2004*a*) for a single inertial mode and the spherical result of Liao & Zhang (2009) (see also Ivers *et al.* 2015). Observe that viscous boundary conditions such as the no-slip condition $\boldsymbol{n} \times \boldsymbol{v} = \boldsymbol{0}$ or the stress-free condition $\boldsymbol{n} \cdot [\nabla \boldsymbol{v} + (\nabla \boldsymbol{v})^{\mathrm{T}}] \times \boldsymbol{n} = \boldsymbol{0}$ on $\partial V$ are not invoked. (Polynomial flows in the spheroid $V$, which satisfy either of these conditions, can be constructed using the toroidal–poloidal fields defined in § 3.1, although not simply in the stress-free case due to coupling of the toroidal and poloidal fields. However, $\boldsymbol{\mathcal{S}}$ does not map such viscous flows to polynomial viscous flows which satisfy the same boundary conditions. Thus, in the spherical limit $a = c$ the toroidal and poloidal no-slip eigenmodes of $\boldsymbol{\mathcal{S}}$ are not polynomials: $t = j_n(j_{n,k}r)Y_n^m(\theta, \phi)$, $s = \{j_n(j_{n+1,k}r) - r^n j_n(j_{n+1,k})\}Y_n^m(\theta, \phi)$; nor are the stress-free modes: $t = j_n(\sigma_{n,k}r)Y_n^m(\theta, \phi)$, $s = \{j_n(\nu_{n,k}r) - r^n j_n(\nu_{n,k})\}Y_n^m(\theta, \phi)$, where $j_{n,k}$, $\sigma_{n,k}$, $\nu_{n,k}$ are the $k$th positive zeros of $j_n(z)$, $zj_n'(z) - j_n(z)$, $2j_{n+1}(z) - zj_n(z)$, respectively. The pressure modes associated with $s$ in each case are $p = -(n+1)j_n(j_{n+1,k})r^n Y_n^m(\theta, \phi)$ and $p = -(n+1)j_n(\nu_{n,k})r^n Y_n^m(\theta, \phi)$.)

The operator $\nabla^2$ can be replaced by the three operators $\partial^2/\partial x^2$, $\partial^2/\partial y^2$, $\partial^2/\partial z^2$. For aligned rotation $\boldsymbol{\mathcal{P}}_N$ splits into a direct sum of rotationally invariant polynomial subspaces for each azimuthal wavenumber $m$ and the operator $\nabla^2$ can be replaced by $(1/s)(\partial/\partial s)(s\partial/\partial s)$, $(1/s^2)\partial^2/\partial\phi^2$, $\partial^2/\partial z^2$. Similarly, the interaction of three Coriolis modes in the advection operator yields $(\boldsymbol{v}_\alpha \cdot \nabla \boldsymbol{v}_\beta, \boldsymbol{v}_\gamma) = 0$ if $\deg\alpha + \deg\beta < \deg\gamma + 1$.

The mapping between Coriolis bases $\boldsymbol{v}_\alpha(\boldsymbol{\Omega}_i)$ with different rotations $\boldsymbol{\Omega}_i$, $i = 1, 2$ can be expressed in the form, $\boldsymbol{v}_\alpha(\boldsymbol{\Omega}_1) = \sum_{deg\beta \leqslant deg\alpha} (\boldsymbol{v}_\alpha(\boldsymbol{\Omega}_1), \boldsymbol{v}_\beta(\boldsymbol{\Omega}_2))\, \boldsymbol{v}_\beta(\boldsymbol{\Omega}_2)$. The non-zero matrix elements of the transformation with respect to the bases $\boldsymbol{v}_\alpha(\boldsymbol{\Omega}_1)$ and $\boldsymbol{v}_\beta(\boldsymbol{\Omega}_2)$ are $(\boldsymbol{v}_\alpha(\boldsymbol{\Omega}_1), \boldsymbol{v}_\beta(\boldsymbol{\Omega}_2))$ with $\deg\beta \leqslant \deg\alpha$. The matrix is unitary, since the Coriolis bases are orthonormal.

## 6. Completeness of the spheroidal Coriolis modes

In this section we establish in Theorem 6.1 the most important result in the paper, that the Coriolis modes in a spheroid are complete in $\boldsymbol{\mathcal{V}}^1(V)$. The proof relies on the uniform polynomial approximation theorem of Weierstrass to approximate a flow in $\boldsymbol{\mathcal{V}}^1(V)$ by a polynomial vector field and the fundamental Theorem 4.3 to project this polynomial field onto $\boldsymbol{\mathcal{P}}_N(V)$ for sufficiently high degree $N$ by subtracting a pressure gradient.

THEOREM 6.1. *The Coriolis modes in a spheroid $V$ are complete in $\boldsymbol{\mathcal{V}}^1(V)$.*

*Proof.* An outline of the proof, which is the same as the spherical one (Ivers *et al.* 2015), is given. Let $\boldsymbol{v} \in \boldsymbol{\mathcal{V}}^1(V)$. Let $\epsilon > 0$. By application of the Weierstrass approximation theorem to each Cartesian component of $\boldsymbol{v}$, there exists an integer $N > 0$ and a vector polynomial $\boldsymbol{u} \in \mathcal{P}_N^3$, such that $|\boldsymbol{v} - \boldsymbol{u}| < \epsilon$ in $V$. However, $\boldsymbol{u}$ is not necessarily in $\boldsymbol{\mathcal{P}}_N$, since $\nabla \cdot \boldsymbol{u} = 0$ in $V$ and $\boldsymbol{n} \cdot \boldsymbol{u} = 0$ on $\partial V$ do not necessarily hold. By Theorem 4.3 there exists a polynomial $\pi \in \mathcal{P}_{N+1}$ such that $\boldsymbol{u} - \nabla\pi \in \boldsymbol{\mathcal{P}}_N$. Hence there are constants $u_k$ such that

$$\boldsymbol{u} = \nabla\pi + \sum_k u_k \boldsymbol{v}_k = \nabla\pi + \sum_k \langle \boldsymbol{u}, \boldsymbol{v}_k \rangle \boldsymbol{v}_k, \tag{6.1}$$

where the $\boldsymbol{v}_k$ are the orthonormal inertial (and geostrophic) modes in $\boldsymbol{\mathcal{P}}_N(V)$. From Ivers *et al.* (2015),

$$\|\boldsymbol{v} - \sum_k \langle \boldsymbol{v}, \boldsymbol{v}_k \rangle \boldsymbol{v}_k\|^2 \leqslant \|\boldsymbol{v} - \boldsymbol{u}\|^2 + \|\nabla\pi\| \|\boldsymbol{v} - \boldsymbol{u}\|. \tag{6.2}$$

https://doi.org/10.1017/jfm.2017.669 Published online by Cambridge University Press

Since $\|\nabla\pi\| \leqslant \|\boldsymbol{u}\|$ and $|\boldsymbol{u}-\boldsymbol{v}| \leqslant \epsilon$ imply $\|\nabla\pi\| \leqslant \|\boldsymbol{v}\| + \epsilon\sqrt{|V|}$, it follows that

$$\|\boldsymbol{v} - \sum_k \langle \boldsymbol{v}, \boldsymbol{v}_k\rangle \boldsymbol{v}_k\|^2 \leqslant \sqrt{|V|}(\|\boldsymbol{v}\| + 2\epsilon\sqrt{|V|})\epsilon. \tag{6.3}$$

The right-hand side is independent of $N$, $\boldsymbol{u}$ and $\pi$ and hence

$$\boldsymbol{v} = \sum_{k=1}^{\infty} \langle \boldsymbol{v}, \boldsymbol{v}_k\rangle \boldsymbol{v}_k \tag{6.4}$$

in an $L^2$ sense. The Coriolis modes are therefore complete in a spheroid. □

We showed that the aligned Coriolis modes are polynomials by construction in § 4. There are no missed eigenfunctions by Ivers *et al.* (2015)

THEOREM 6.2. *The spheroidal Coriolis modes are polynomials.*

## 7. Conclusions

It has been shown that the solution of the polynomial Poisson–Neumann problem, i.e. Poisson's equation with Neumann boundary condition and polynomial data, in a spheroid is a polynomial. This fundamental result has been used to show that the Coriolis operator $\mathcal{C}$ is a skew-symmetric bounded linear operator which maps incompressible polynomial flows of degree $N$ or less in a spheroid to incompressible polynomial flows of degree $N$ or less. In fact, $\mathcal{C}$ maps flows to flows of the same degree. The eigenmodes (inertial and geostrophic modes) of $\mathcal{C}$, which are tilted if the rotation axis is not aligned with the symmetry axis of the spheroid, form an orthogonal basis for the finite-dimensional space of spheroidal polynomial flows. This property enabled enumeration of the modes and proof of their completeness using the Weierstrass polynomial approximation theorem. The Coriolis modes of degree one and all geostrophic modes have been explicitly constructed. It has also been shown that only the Coriolis modes of degree one have non-zero angular momentum in the boundary frame.

The computation of tilted inertial modes and their analytical forms require lengthy mathematical backgrounds, particularly the analytic treatment of the pressure boundary condition (1.14) ($\boldsymbol{f} = \boldsymbol{0}$), and will be considered in future work.

## REFERENCES

ALDRIDGE, K. D. & LUMB, L. I. 1987 Inertial waves identified in the Earth's fluid outer core. *Nature* **325**, 421–423.

ALDRIDGE, K. D. & TOOMRE, A. 1969 Axisymmetric inertial oscillations of a fluid in a rotating spherical container. *J. Fluid Mech.* **37**, 307–323.

BACKUS, G. & RIEUTORD, M. 2017 Completeness of inertial modes of an incompressible inviscid fluid in a corotating ellipsoid. *Phys. Rev.* E **95**, 053116.

BALICK, B. & FRANK, A. 2002 Shapes and shaping of planetary nebulae. *Annu. Rev. Astron. Astrophys.* **40**, 439–486.

BRYAN, G. H. 1889 The waves on a rotating liquid spheroid of finite ellipticity. *Phil. Trans. R. Soc. Lond.* A **180**, 187–219.

CHAN, K. H., LIAO, X. & ZHANG, K. 2011 Simulations of fluid motion in spheroidal planetary cores driven by latitudinal libration. *Phys. Earth Planet. Inter.* **187**, 404–415.

https://doi.org/10.1017/jfm.2017.669 Published online by Cambridge University Press

CUI, Z., ZHANG, K. & LIAO, X. 2014 On the completeness of inertial wave modes in rotating annular channels. *Geophys. Astrophys. Fluid Dyn.* **108**, 44–59.

DERMOTT, S. F. 1979 Shapes and gravitational moments of satellites and asteroids. *Icarus* **37**, 575–586.

DYSON, J. & SCHUTZ, P. F. 1979 Perturbations and stability of rotating stars. I. Completeness of normal modes. *Proc. R. Soc. Lond.* A **368**, 389–410.

GANS, R. F. 1970 On the hydromagnetic precession in a cylinder. *J. Fluid Mech.* **45**, 111–130.

GREENSPAN, H. P. 1968 *The Theory of Rotating Fluids*. Cambridge University Press.

HOUGH, S. S. 1895 The oscillations of a rotating ellipsoidal shell containing fluid. *Phil. Trans. R. Soc. Lond.* A **186**, 469–506.

IVANOV, P. B. & PAPALOIZOU, J. C. B. 2010 Inertial waves in rotating bodies: a WKBJ formalism for inertial modes and a comparison with numerical results. *Mon. Not. R. Astron. Soc.* **407**, 1609–1630.

IVERS, D. J. 2017*a* Enumeration, orthogonality and completeness of the incompressible Coriolis modes in a tri-axial ellipsoid. *Geophys. Astrophys. Fluid Dyn.* **111**, 333–354.

IVERS, D. J. 2017*b* Kinematic dynamos in spheroidal geometries. *Proc. R. Soc. Lond.* A **473**, 20170432.

IVERS, D. J., JACKSON, A. & WINCH, D. 2015 Enumeration, orthogonality and completeness of the incompressible Coriolis modes in a sphere. *J. Fluid Mech.* **766**, 468–498.

KELLEY, D. H., TRIANA, S. A., ZIMMERMAN, D. S., TILGNER, A. & LATHROP, D. P. 2007 Inertial waves driven by differential rotation in a planetary geometry. *Geophys. Astrophys. Fluid Dyn.* **101**, 469–487.

KERSWELL, R. R. 1993 The instability of precessing flow. *Geophys. Astrophys. Fluid Dyn.* **72**, 107–144.

KERSWELL, R. R. 1994 Tidal excitation of hydromagnetic waves and their damping in the earth. *J. Fluid Mech.* **214**, 219–241.

KUDLICK, M. D. 1966 On transient motions in a contained rotating fluid. PhD thesis, MIT.

LE BARS, M., DIZÈS, S. L. & LE GAL, P. 2007 Coriolis effects on the elliptical instability in cylindrical and spherical rotating containers. *J. Fluid Mech.* **585**, 323–342.

LEBOVITZ, N. R. 1989 The stability equations for rotating, inviscid fluids: Galerkin methods and orthogonal bases. *Geophys. Astrophys. Fluid Dyn.* **46**, 221–243.

LIAO, X. & ZHANG, K. 2009 A new integral property of inertial waves in rotating fluid spheres. *Proc. R. Soc. Lond.* A **465**, 1075–1091.

LIAO, X. & ZHANG, K. 2010*a* Asymptotic and numerical solutions of the initial value problem in rotating planetary fluid cores. *Geophys. J. Intl* **180**, 181–192.

LIAO, X. & ZHANG, K. 2010*b* A new Legendre-type polynomial and its application to geostrophic flow in rotating fluid spheres. *Proc. R. Soc. Lond.* A **466**, 2203–2217.

LORENZANI, S. & TILGNER, A. 2003 Inertial instabilities of fluid flow in precessing spheroidal shells. *J. Fluid Mech.* **492**, 363–379.

MACROBERT, T. M. 1947 *Spherical Harmonics: An Elementary Treatise on Harmonic Functions with Applications*, 2nd edn. Methuen.

MAFFEI, S., JACKSON, A. & LIVERMORE, P. W. 2017 Characterization of columnar inertial modes in rapidly rotating spheres and spheroids. *Proc. R. Soc. Lond.* A **473**, 20170181.

MALKUS, W. V. R. 1967 Hydromagnetic planetary waves. *J. Fluid Mech.* **28**, 793–802.

NOIR, J., HEMMERLIN, F., WICHT, J., BACA, S. M. & AURNOU, J. M. 2009 An experimental and numerical study of librationally driven flow in planetary cores and subsurface oceans. *Phys. Earth Planet. Inter.* **173**, 141–152.

OGILVIE, G. I. & LIN, D. N. C. 2004 Tidal dissipation in rotating giant planets. *Astrophys. J.* **610**, 477–509.

POINCARÉ, H. 1885 Sur l'équilibre d'une masse fluide animée d'un mouvement de rotation. *Acta Math.* **7**, 259–380.

SCHMITT, D. 2006 Numerical study of viscous modes in a rotating spheroid. *J. Fluid Mech.* **567**, 399–414.

https://doi.org/10.1017/jfm.2017.669 Published online by Cambridge University Press

SCHMITT, D. & JAULT, D. 2004 Numerical study of a rotating fluid in a spheroidal container. *J. Comput. Phys.* **197**, 671–685.

STACEY, F. D. & DAVIS, P. M. 2008 *Physics of the Earth*, 4th edn. Cambridge University Press.

TASSOUL, J. L. 1978 *Theory of Rotating Stars*. Princeton University Press.

THOMAS, P. C. 2010 Sizes, shapes, and derived properties of the saturnian satellites after the Cassini nominal mission. *Nature* **208**, 395–401.

THOMSON, W. 1880 Vibrations of a columnar vortex. *Phil. Mag.* **10**, 155–168.

TILGNER, A. 2007 Zonal wind driven by inertial modes. *Phys. Rev. Lett.* **99**, 194501.

VANTIEGHEM, S. 2014 Inertial modes in a rotating triaxial ellipsoid. *Proc. R. Soc. Lond.* A **470**, 20140093.

WU, C. C. & ROBERTS, P. H. 2011 High order instabilities of the Poincaré solution for precessionally driven flow. *Geophys. Astrophys. Fluid Dyn.* **105**, 287–303.

ZHANG, K. 1993 On equatorially trapped boundary inertial waves. *J. Fluid Mech.* **248**, 203–217.

ZHANG, K. 1994 On coupling between the Poincaré equation and the heat equation. *J. Fluid Mech.* **268**, 211–229.

ZHANG, K. 1995 On coupling between the Poincaré equation and the heat equation: non-slip boundary condition. *J. Fluid Mech.* **284**, 239–256.

ZHANG, K., CHAN, K. H. & LIAO, X. 2014 On precessing flow in an oblate spheroid of arbitrary eccentricity. *J. Fluid Mech.* **743**, 358–384.

ZHANG, K., EARNSHAW, P., LIAO, X. & BUSSE, F. H. 2001 On inertial waves in a rotating fluid sphere. *J. Fluid Mech.* **437**, 103–119.

ZHANG, K. & LIAO, X. 2004 A new asymptotic method for the analysis of convection in a rapidly rotating sphere. *J. Fluid Mech.* **518**, 319–346.

ZHANG, K. & LIAO, X. 2017 *Theory and Modeling of Rotating Fluids: Convection, Inertial Waves and Precession*. Cambridge University Press.

ZHANG, K., LIAO, X. & EARNSHAW, P. 2004*a* On inertial waves and oscillations in a rapidly rotating spheroid. *J. Fluid Mech.* **504**, 1–40.

ZHANG, K., LIAO, X. & EARNSHAW, P. 2004*b* The Poincaré equation: a new polynomial and its unusual properties. *J. Math. Phys.* **45**, 4777–4790.

https://doi.org/10.1017/jfm.2017.669 Published online by Cambridge University Press